Sterile neutrinos in $\Lambda_b^0 \to (\Lambda_c^+, p^+)\ell_1^-\ell_2^-\ell_3^+\nu$ decays

Diganta Das[1,*] and Jaydeb Das[2,†]

[1]*Center for Computational Natural Sciences and Bioinformatics, International Institute of Information Technology, Hyderabad 500 032, India*

[2]*Department of Physics and Astrophysics, University of Delhi, Delhi 110007, India*

(Received 5 September 2021; accepted 4 January 2022; published 13 January 2022)

We study lepton number violating and lepton number conserving semileptonic decays of heavy baryons Λ_b^0 to three charged leptons and a neutrino. The decays occur through two intermediate quasidegenerate GeV-scale sterile neutrinos of either Majorana or Dirac type that can be on-shell. Interference between the intermediate heavy neutrinos leads to CP violation in the final states. Effect of neutrino oscillations between the heavy states are also considered in observables of interests, i.e., branching ratio, and the CP-asymmetry. Given the present constraints on the heavy-to-light mixing elements $|V_{eN}|$ and $|V_{\mu N}|$, CP-averaged branching ratio of $\Lambda_b^0 \to (\Lambda_c, p)\mu\mu e\nu$ with intermediate Majorana neutrinos is almost two orders of magnitude larger than for the same with Dirac neutrinos, whereas, CP-averaged branching ratio of $\Lambda_b^0 \to (\Lambda_c, p)ee\mu\nu$ is of the same order of magnitude for both Majorana and Dirac neutrino induced decays. CP-violation is found to be appreciable when the neutrino mass difference is comparable with the average decay widths.

DOI: 10.1103/PhysRevD.105.013009

I. INTRODUCTION

It is now confirmed from neutrino oscillation experiments that active light neutrinos have mass [1–3], albeit very tiny. The reason for the smallness is yet unknown, but the very existence of neutrino mass may indicate the existence of a right-handed gauge-singlet (sterile) counterpart N_R. Whether the N_R is of the Dirac or Majorana type is a crucial question and is intricately related to the question of the origin of neutrino mass itself. If N_R is a Dirac type then, tree-level Dirac neutrino mass terms are allowed, but it leads to an unnaturally small Yukawa coupling for neutrinos. If the N_R is a Majorana, then both Dirac type mass term $m_D(\bar{\nu}_L N_R + \text{H.c.})$ and Majorana term $m_N N_R N_R$ are allowed by the SM. Then, small light neutrino mass $m_\nu \sim m_D^2/m_N$, where m_D is at the electroweak scale or lower, arise through "seesaw" mechanism [4–10]. There are several versions of the mechanism. In type-I seesaw, the masses of N_R are of the order of a few TeV which leads to $m_\nu \lesssim 1$ eV. Recently, low energy seesaw mechanism has been proposed where N_R have a mass of the order few hundreds of MeV to a few GeV [11–18]. These GeV-scale seesaw mechanisms can be experimentally accessed at the intensity and the energy frontier.

Majorana neutrinos distinguish themselves from Dirac through $|\Delta L| = 2$ lepton number violating (LNV) processes. Neutrinoless double beta decay ($0\nu\beta\beta$) process is highly sensitive probe of LNV process for light Majorana exchange [19–22] but enhancement due to GeV-scale Majorana has recently been shown [23,24]. Due to the lack of any $0\nu\beta\beta$ processes so far, and due to its limitations to probe LNV in the first neutrino family only, alternative processes are highly desirable. Majorana neutrino-mediated rare decays of mesons and baryons are useful in this regard. Interestingly, if Majorana neutrinos exist in nature, then it will lead to both LNV as well as lepton-number-conserving (LNC) decays of hadrons. The LNC decays are not unique to Majorana neutrinos and occur through Dirac neutrino exchange as well. The aim of this paper is to study LNV and LNC in Λ_b^0 baryonic decays. Usually, for a too light or a too heavy sterile neutrino, decay rates are too suppressed to be observed in the current experiments. But, if the sterile neutrino masses are within a few hundreds of MeV to a few GeV, then they can go on-shell resulting in appreciable decay rates [25,26]. A number of searches of Majorana neutrino mediated LNV decays are underway at the LHC and Belle-II which has renewed its interests in the theoretical aspects including in hadronic decays [25–59], τ-lepton decays [60–65], and different scattering processes [66–76]. Experimentally, the $B^- \to \pi^+\mu^-\mu^-$ decay has been searched by the LHCb [77] and the $K^- \to \pi^+\mu^-\mu^-$ decay has been searched by the NA48/2 Collaborations [78]

*diganta.das@iiit.ac.in
†jaydebphysics@gmail.com

and these measurements give the stringent constraints on the heavy-to-light mixing elements. With large integrated luminosity expected at the future Belle-II as well as at the LHC in the future upgrade, the sensitivity of sterile neutrinos to hadronic decays is expected to increase.

In this paper we study the rare decay processes $\Lambda_b^0 \to (\Lambda_c^+, p^+)\ell_1^-\ell_2^-\ell_3^+\nu$ and their conjugate modes where ℓ_1, ℓ_2, ℓ_3 can in general be of different flavors. The decays are induced by sterile neutrinos that can be either of Majorana or Dirac types. Two sterile neutrinos N_j $(j = 1, 2)$ with masses m_{N_1} and m_{N_2} in the range of a few hundreds of MeV to a few GeV are considered. In these mass ranges, the neutrinos can go on-shell, i.e., decay widths $\Gamma_{N_j} \ll m_{N_j}$. We are interested in scenarios where the two neutrinos are almost degenerate, i.e., $\Delta M_N \equiv m_{N_1} - m_{N_2} \ll m_{N_1}, m_{N_2}$. Models with quasidegenerate Majorana neutrinos with mass in this range have been proposed in Ref. [79]. If the sterile neutrinos are Majorana then both LNV and LNC final states will result. If the sterile neutrinos are Dirac, only LNC final state will result. Irrespective of the nature of the neutrinos involved, CP violation is expected for both types of neutrinos. In this paper, we present the expression for the branching ratios for both the LNV and the LNC cases. We note that LNV decays of hyperons are of experimental interest and have been searched by several experimental collaborations in Ξ, Λ_c and Σ decays [80–82]. We are not aware of such searches in Λ_b^0 decays. Theoretically, only Majorana neutrino induced LNV decays in $\Lambda_b^0 \to (\Lambda_c^+, p^+)\pi^+\mu^-\mu^-$ decays were studied in Refs. [38,59] where neutrinos oscillation effects were neglected. In this paper, we also include the effect of neutrinos oscillation in the expressions of the branching ratios.

We present CP-averaged branching ratios for $\Delta M_N \sim \Gamma_N$, where $\Gamma_N = (\Gamma_{N_1} + \Gamma_{N_2})/2$ is the average decay width. Due to CKM suppression, $\Lambda_b^0 \to p\ell_1\ell_2\ell_3\nu$ has a smaller branching ratio than $\Lambda_b^0 \to \Lambda_c\ell_1\ell_2\ell_3\nu$. When the decays occur through intermediate Majorana neutrinos, branching ratio of $\Lambda_b^0 \to (\Lambda_c, p)ee\mu\nu$ is at least two orders of magnitude suppressed compared to $\Lambda_b^0 \to (\Lambda_c, p)\mu\mu e\nu$ due to present experimental upper bounds on the heavy to light mixing elements $|V_{\mu N}|^2 < 10^{-5}$, $|V_{eN}|^2 < 10^{-7}$. On the other hand, when the decays occur through intermediate Dirac neutrinos, the CP average branching ratios of $\Lambda_b^0 \to (\Lambda_c, p)\mu\mu e\nu$ and $\Lambda_b^0 \to (\Lambda_c, p)ee\mu\nu$ are of the same order of magnitude. Comparing Majorana and Dirac neutrino induced decays, we find that for $\Lambda_b^0 \to (\Lambda_c, p)\mu\mu e\nu$ the branching ratio with intermediate Majorana is almost two orders of magnitude larger than that with intermediate Dirac. But for the $\Lambda_b^0 \to (\Lambda_c, p)ee\mu\nu$ the branching ratios are of the same order of magnitude for Majorana and Dirac cases. The CP-asymmetry is sensitive to the heavy neutrino displaced vertex length L, and maximum CP-violation is obtained in the region where the CP-odd phase is $\pi/2$, $\Delta M_N \sim \Gamma_N$, and $L \sim L_{\rm osc}$, where $L_{\rm osc}$ is the heavy neutrino oscillation length. For large values of L, the CP-violation is suppressed.

The paper is organized as follows. In Sec. II we give a generic formalism including neutrino oscillation for the case of $\mathcal{B}_1 \to \mathcal{B}_2\ell_1^-\ell_2^-\ell_3^+\nu$ and its CP conjugate mode $\bar{\mathcal{B}}_1 \to \bar{\mathcal{B}}_2\ell_1^+\ell_2^+\ell_3^-\bar{\nu}$ mediated by degenerate on-shell both Majorana and Dirac neutrinos. In Sec. III we perform the numerical analysis and the results are summarized in Sec. IV. Some details of our derivations are given in the Appendixes.

II. FORMALISM

Our calculations are based on a model where the left-handed neutrinos of the SM $SU(2)$ doublets are accompanied by two right-handed sterile neutrinos N_1 and N_2. The relation between the SM flavor eigenstates $\nu_{\ell_i L}$ and the mass eigenstates $\nu_{i,L}, N_1, N_2$ is

$$\nu_{\ell_i L} = \sum_{i=1}^{3} V_{\ell_i\nu_j}\nu_{j,L} + V_{\ell_i N_1}N_1 + V_{\ell_i N_2}N_2, \quad \ell_i = e^-, \mu^-, \tau^-. \tag{2.1}$$

The heavy to light mixing elements $V_{\ell_i N_1}$ and $V_{\ell_i N_2}$ are the free parameters of our model which can be constrained by

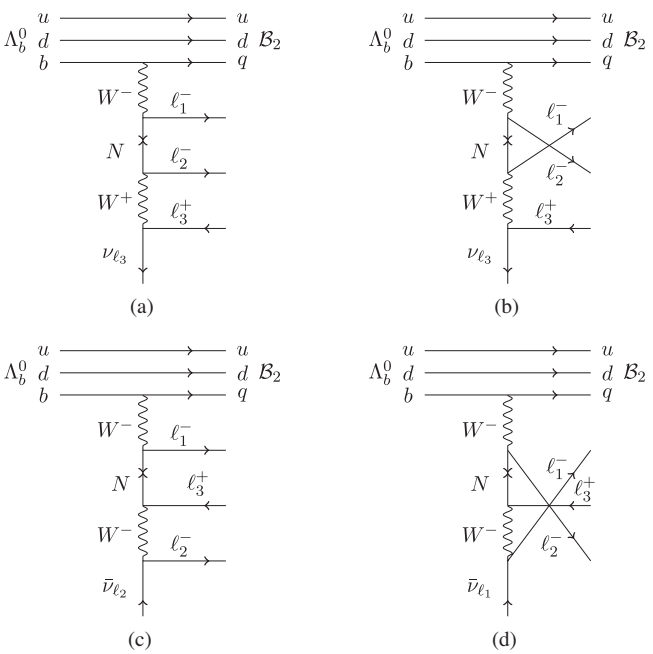

FIG. 1. Figure (a) and (b) represent the LNV processes for direct and crossed channel diagram respectively. Figure (c) and (d) represent the LNC processes for direct and crossed channel Feynman diagram respectively. Here q is the charm and up quark for $\mathcal{B}_2 = \Lambda_c^+$ and proton (p^+) respectively.

experimental data. The parameters in general can be complex. We assume a convention that $V_{\ell_i N_j}$ is the mixing between a negatively charged lepton and a sterile neutrino and define a CP-odd phase $\phi_{\ell_i N_j}$ as

$$V_{\ell_i N_j} = |V_{\ell_i N_j}| e^{i\phi_{\ell_i N_j}}, \quad j = 1, 2 \tag{2.2}$$

Under the assumption of CPT conservation, a Majorana neutrino differs from a Dirac neutrino in the fact that the former needs only two degrees of freedom (two helicities) compared to the latter's four (two helicities each for particle and antiparticle). Another important difference between the two lies in how the PMNS mixing matrix is parametrized for them. For Dirac neutrinos, the PMNS matrix can be parametrized in terms of three mixing angles and one CP-violating phase which is called the Dirac phase [83]. For Majorana neutrinos, two additional CP phases, called Majorana phases, are needed.

Our interest is to calculate $\Lambda_b^0 \to (\Lambda_c^+, p^+)\ell_1^-\ell_2^-\ell_3^+\nu$ decays and their conjugate modes. Depending on the flavor of the neutrinos that are unobserved, the decays can be either LNV or LNC. For example, $\Lambda_b^0 \to (\Lambda_c^+, p^+)\ell_1^-\ell_2^-\ell_3^+\nu$ is LNV if ν is ν_{ℓ_3}, but it is LNC if ν is $\bar{\nu}_{\ell_2}$. The LNV decays occur due to Majorana neutrinos whereas LNC decays can happen either due to Majorana or a Dirac.[1] At the LHC, the reconstruction efficiency of tau leptons are is smaller than muon and electrons. Moreover, the tau leptons in the final state are also expected to give severe phase space suppressions. For these reasons, we neglect tau leptons. To reduce the dominant electromagnetic backgrounds we also avoid the events where two leptons of opposite charges are present. Therefore, we will study only the following combinations of leptons in the $\Lambda_b^0 \to (\Lambda_c^+, p^+)\ell_1^-\ell_2^-\ell_3^+\nu$ decays. Depending on the flavor of the unobserved neutrinos the final states can be either LNV or LNC.

$$\begin{aligned}
&\text{LNV:}\ (i)\ \ell_1 = \ell_2 = \mu, \quad \ell_3 = e, \nu = \nu_{\ell_3}; \quad (ii)\ \ell_1 = \ell_2 = e, \quad \ell_3 = \mu, \quad \nu = \nu_{\ell_3} \\
&\text{LNC:}\ (i)\ \ell_1 = \ell_2 = \mu, \quad \ell_3 = e, \nu = \bar{\nu}_{\ell_2}; \quad (ii)\ \ell_1 = \ell_2 = e, \quad \ell_3 = \mu, \quad \nu = \bar{\nu}_{\ell_2}
\end{aligned}$$

To clarify our convention, when the decay is LNV, the ℓ_1, ℓ_2 are assumed attached to the vertexes of the sterile neutrino and the $\ell_3\nu$ pair comes from a W. When the decay is LNC, the ℓ_1, ℓ_3 are assumed attached to the vertices of the sterile neutrino and the $\ell_2\nu$ pair comes from a W. The Feynman diagrams for these relevant processes are shown in Fig. 1. The dominant contributions come from two "s-channel" topologies, direct(D), and cross-channel. There are no "t-channel" diagrams for these processes. The decay rates are appreciable if the sterile neutrinos have kinematically allowed masses

$$\begin{aligned}
&m_{\ell_2} + m_{\ell_3} < m_{N_j} < (m_{\mathcal{B}1} - m_{\mathcal{B}2} - m_{\ell_1}), \quad \text{and/or} \\
&m_{\ell_1} + m_{\ell_3} < m_{N_j} < (m_{\mathcal{B}1} - m_{\mathcal{B}2} - m_{\ell_2}).
\end{aligned} \tag{2.3}$$

A. $\mathcal{B}_1 \to \mathcal{B}_2\ell_1 N \to \mathcal{B}_2\ell_1\ell_2\ell_3\nu$ rates

The five-body decay can be viewed as a two-step process, production of the heavy neutrino in the semileptonic decay $\mathcal{B}_1 \to \mathcal{B}_2\ell_1 N$, followed by the decay of the heavy neutrino $N \to \ell_2\ell_3\nu$. With a Majorana neutrino being exchanged, the process will be LNV and the decay rates can be written as [59]

$$\begin{aligned}
\Gamma^{\rm LNV}_{\mathcal{B}_1} \equiv \Gamma(\mathcal{B}_1 \to \mathcal{B}_2\ell_1^-\ell_2^-\ell_3^+\nu_{\ell_3}) = (2 - \delta_{\ell_1\ell_2})\frac{1}{2!}[&|V_{\ell_1 N_1}|^2|V_{\ell_2 N_1}|^2(\hat{\Gamma}(DD^*)_{11} + \hat{\Gamma}(CC^*)_{11}) \\
&+ |V_{\ell_1 N_2}|^2|V_{\ell_2 N_2}|^2(\hat{\Gamma}(DD^*)_{22} + \hat{\Gamma}(CC^*)_{22}) \\
&+ 2|V_{\ell_1 N_1}||V_{\ell_2 N_1}||V_{\ell_1 N_2}||V_{\ell_2 N_2}|\{\cos(\theta_{21}^{\rm LNV})({\rm Re}\hat{\Gamma}(DD^*)_{12} + {\rm Re}\hat{\Gamma}(CC^*)_{12}) \\
&+ \sin(\theta_{21}^{\rm LNV})({\rm Im}\hat{\Gamma}(DD^*)_{12} + {\rm Im}\hat{\Gamma}(CC^*)_{12})\}],
\end{aligned} \tag{2.4}$$

$$\begin{aligned}
\Gamma^{\rm LNV}_{\bar{\mathcal{B}}_1} \equiv \Gamma(\bar{\mathcal{B}}_1 \to \bar{\mathcal{B}}_2\ell_1^+\ell_2^+\ell_3^-\bar{\nu}_{\ell_3}) = (2 - \delta_{\ell_1\ell_2})\frac{1}{2!}[&|V_{\ell_1 N_1}|^2|V_{\ell_2 N_1}|^2(\hat{\Gamma}(DD^*)_{11} + \hat{\Gamma}(CC^*)_{11}) \\
&+ |V_{\ell_1 N_2}|^2|V_{\ell_2 N_2}|^2(\hat{\Gamma}(DD^*)_{22} + \hat{\Gamma}(CC^*)_{22}) \\
&+ 2|V_{\ell_1 N_1}||V_{\ell_2 N_1}||V_{\ell_1 N_2}||V_{\ell_2 N_2}|\{\cos(\theta_{21}^{\rm LNV})({\rm Re}\hat{\Gamma}(DD^*)_{12} + {\rm Re}\hat{\Gamma}(CC^*)_{12}) \\
&- \sin(\theta_{21}^{\rm LNV})({\rm Im}\hat{\Gamma}(DD^*)_{12} + {\rm Im}\hat{\Gamma}(CC^*)_{12})\}].
\end{aligned} \tag{2.5}$$

[1]We neglect contributions of the Standard Model light neutrinos since the decays under consideration can not occur through their on-shell production and the decay rates are suppressed by the light neutrino masses. This is true irrespective of whether the light neutrinos are of the Dirac or Majorana type.

Based on the convention (2.2)

$$\begin{aligned}\theta_{21}^{\rm LNV} &= \arg(V_{\ell_1 N_2}) + \arg(V_{\ell_2 N_2}) - \arg(V_{\ell_1 N_1}) - \arg(V_{\ell_2 N_1}),\\ &= (\phi_{\ell_1 N_2} + \phi_{\ell_2 N_2} - \phi_{\ell_1 N_1} - \phi_{\ell_2 N_1}),.\end{aligned} \tag{2.6}$$

The LNC finals state can result either due to Majorana or Dirac neutrinos. The expression of LNC rates are

$$\begin{aligned}\Gamma_{\mathcal{B}_1}^{\rm LNC} \equiv \Gamma(\mathcal{B}_1 \to \mathcal{B}_2 \ell_1^- \ell_2^- \ell_3^+ \bar{\nu}_{\ell_2}) &= (2-\delta_{\ell_1\ell_2})\frac{1}{2!}[|V_{\ell_1 N_1}|^2 |V_{\ell_3 N_1}|^2 (\hat{\Gamma}(DD^*)_{11} + \kappa_1^2 \hat{\Gamma}(CC^*)_{11})\\ &+ |V_{\ell_1 N_2}|^2 |V_{\ell_3 N_2}|^2 (\hat{\Gamma}(DD^*)_{22} + \kappa_2^2 \hat{\Gamma}(CC^*)_{22})\\ &+ 2|V_{\ell_1 N_1}||V_{\ell_3 N_1}||V_{\ell_1 N_2}||V_{\ell_3 N_2}|\{\cos(\theta_{21}^{\rm LNC})({\rm Re}\hat{\Gamma}(DD^*)_{12} + \kappa_1\kappa_2 {\rm Re}\hat{\Gamma}(CC^*)_{12})\\ &+ \sin(\theta_{21}^{\rm LNC})({\rm Im}\hat{\Gamma}(DD^*)_{12} + \kappa_1\kappa_2 {\rm Im}\hat{\Gamma}(CC^*)_{12})\}],\end{aligned} \tag{2.7}$$

$$\begin{aligned}\Gamma_{\bar{\mathcal{B}}_1}^{\rm LNC} \equiv \Gamma(\bar{\mathcal{B}}_1 \to \bar{\mathcal{B}}_2 \ell_1^+ \ell_2^+ \ell_3^- \nu_{\ell_2}) &= (2-\delta_{\ell_1\ell_2})\frac{1}{2!}[|V_{\ell_1 N_1}|^2 |V_{\ell_3 N_1}|^2 (\hat{\Gamma}(DD^*)_{11} + \kappa_1^2 \hat{\Gamma}(CC^*)_{11})\\ &+ |V_{\ell_1 N_2}|^2 |V_{\ell_3 N_2}|^2 (\hat{\Gamma}(DD^*)_{22} + \kappa_2^2 \hat{\Gamma}(CC^*)_{22})\\ &+ 2|V_{\ell_1 N_1}||V_{\ell_3 N_1}||V_{\ell_1 N_2}||V_{\ell_3 N_2}|\{\cos(\theta_{21}^{\rm LNC})({\rm Re}\hat{\Gamma}(DD^*)_{12} + \kappa_1\kappa_2 {\rm Re}\hat{\Gamma}(CC^*)_{12})\\ &- \sin(\theta_{21}^{\rm LNC})({\rm Im}\hat{\Gamma}(DD^*)_{12} + \kappa_1\kappa_2 {\rm Im}\hat{\Gamma}(CC^*)_{12})\}].\end{aligned} \tag{2.8}$$

The expressions of $\hat{\Gamma}(XX^*)$ are different for LNV and LNC rates and have been derived in Appendix A. The factor $1/2!$ in the decay rates is the combinatorial factor when to account for the scenario when two charged leptons in the final state are the same. The CP-odd phase $\theta_{21}^{\rm LNC}$, and $\kappa_{1,2}$ are defined as

$$\begin{aligned}\theta_{21}^{\rm LNC} &= \arg(V_{\ell_1 N_2}) - \arg(V_{\ell_3 N_2}) - \arg(V_{\ell_1 N_1}) + \arg(V_{\ell_3 N_1}),\\ &= (\phi_{\ell_1 N_2} - \phi_{\ell_3 N_2} - \phi_{\ell_1 N_1} + \phi_{\ell_3 N_1}),\\ \kappa_1 &= \frac{|V_{\ell_2 N_1}|}{|V_{\ell_1 N_1}|}, \qquad \kappa_2 = \frac{|V_{\ell_2 N_2}|}{|V_{\ell_1 N_2}|}\end{aligned} \tag{2.9}$$

In general, the CP-odd phases $\theta_{21}^{\rm LNV}$ and $\theta_{21}^{\rm LNC}$ are different and $\theta_{21}^{\rm LNV}$ is not equal to $\theta_{21}^{\rm LNC}$ by the replacement $\ell_2 \to \ell_3$.

In the decay rate formulas given above, contributions coming from $D-C$ channel interference have been neglected as they are negligibly small. To give some physical interpretation, up to the heavy-to-light mixing elements, the diagonal terms $\hat{\Gamma}(XX^*)_{ij}, X = D, C$ are the decay rates involving ith neutrino in the X channel and jth neutrino in the conjugate channel. The on-shell assumption $\Gamma_{N_j} \ll m_{N_j}$ is always valid in our case, and the diagonal elements can be calculated analytically as

$$\begin{aligned}\hat{\Gamma}(DD^*)_{jj} &= \bar{\Gamma}(\mathcal{B}_1 \to \mathcal{B}_2 \ell_1 N_j) \times \frac{\bar{\Gamma}(N_j \to \ell_2 \ell_3 \nu)}{\Gamma_{N_j}},\\ \hat{\Gamma}(CC^*)_{jj} &= \hat{\Gamma}(DD^*)_{jj}(\ell_1 \leftrightarrow \ell_2),\end{aligned} \tag{2.10}$$

where we have adopted the notation $\Gamma(\mathcal{B}_1 \to \mathcal{B}_2 \ell_1 N_j) = |V_{\ell_1 N}|^2 \bar{\Gamma}(\mathcal{B}_1 \to \mathcal{B}_2 \ell_1 N_j)$ and $\Gamma(N_j \to \ell_2 \ell_3 \nu) = |V_{(\ell_2/\ell_3)N}|^2 \bar{\Gamma}(N_j \to \ell_2 \ell_3 \nu)$. As the neutrinos are almost degenerate we can assume that

$$\begin{aligned}&\bar{\Gamma}(\mathcal{B}_1 \to \mathcal{B}_2 \ell_1 N_1) = \bar{\Gamma}(\mathcal{B}_1 \to \mathcal{B}_2 \ell_1 N_2) \equiv \bar{\Gamma}(\mathcal{B}_1 \to \mathcal{B}_2 \ell_1 N),\\ &\bar{\Gamma}(N_1 \to \ell_2 \ell_3 \nu) = \bar{\Gamma}(N_2 \to \ell_2 \ell_3 \nu) \equiv \bar{\Gamma}(N \to \ell_2 \ell_3 \nu).\end{aligned} \tag{2.11}$$

The differential expressions of the normalized three body decay width $d\bar{\Gamma}(\mathcal{B}_1 \to \mathcal{B}_2 \ell_1 N)$ are given in Appendix B 2 and related three body decay kinematics for this relevant process are given in Appendix B 1. The explicit expression of normalized decay width of heavy sterile neutrino N without heavy to light mixing element, $\bar{\Gamma}(N \to \ell_2 \ell_3 \nu)$ is taken from [57]. The off-diagonal elements ${\rm Re}\hat{\Gamma}(XX^*)_{12}$ and ${\rm Im}\hat{\Gamma}(XX^*)_{12}$ are the ones where the two neutrinos interfere making them sensitive to the mass difference ΔM_N, and hence, on the assumption $\Gamma_{N_j} \ll \Delta M_N$. This sensitivity can be parametrized in terms of $\delta(y)$ and $\eta(y)$ [59]

$$\begin{aligned}\frac{{\rm Re}\hat{\Gamma}(XX^*)_{12}}{\hat{\Gamma}(XX^*)_{jj}} &= 2\delta(y)\frac{\Gamma_{N_j}}{\Gamma_{N_1}+\Gamma_{N_2}},\\ \frac{{\rm Im}\hat{\Gamma}(XX^*)_{12}}{\hat{\Gamma}(XX^*)_{jj}} &= 2\frac{\eta(y)}{y}\frac{\Gamma_{N_j}}{\Gamma_{N_1}+\Gamma_{N_2}}, \quad X = C,D; j = 1,2\end{aligned} \tag{2.12}$$

where $y = \Delta M_N/\Gamma_N$, and $\Gamma_N = (\Gamma_{N_1} + \Gamma_{N_2})/2$ is the average decay width. Numerically we find

$$\eta(y) = \frac{y^2}{y^2+1}, \qquad \delta(y) = \frac{1}{y^2+1}, \tag{2.13}$$

which is in agreement with similar decays in mesons [58]. Physically, $\delta(y)$ and $\eta(y)$ are correction terms for non-negligible overlap of the two neutrinos. In Fig. 2 we show η and δ as a function of y. $\mathrm{Re}\hat{\Gamma}(XX^*)_{12}$ and $\mathrm{Im}\hat{\Gamma}(XX^*)_{12}$ are also sources of a CP-even phase $\Delta\xi = \xi_1 - \xi_2$ where

$$\tan\xi_1 = \frac{m_{N_1}\Gamma_{N_1}}{k_N^2 - m_{N_1}^2}, \qquad \tan\xi_2 = \frac{m_{N_2}\Gamma_{N_2}}{k_N^2 - m_{N_2}^2}. \tag{2.14}$$

where k_N is the momentum of the intermediate neutrinos. The cosine and sine of the angles $\Delta\xi$ come from the $\mathrm{Re}\hat{\Gamma}(XX^*)_{12}$ and $\mathrm{Im}\hat{\Gamma}(XX^*)_{12}$ parts, respectively [59].

We will use the Eqs. (2.10)–(2.12) in the subsequent sections to simplify the decay rates.

B. Neutrino oscillation

In the previous expressions of decay widths, two effects are missing, acceptance factor P_N, which is a probability that the sterile neutrino decays within the detector in its flight, and the oscillation between N_1 and N_2 states. The effect of heavy neutrino oscillation is that the decay rates depend on the length of flight L of the heavy neutrinos between production and decay vertex [44]. The acceptance factors is given by

$$P_{N_j} = 1 - \exp\left(-\frac{t}{\tau_{N_j}\gamma_{N_j}}\right) = 1 - \exp\left(-\frac{L\Gamma_{N_j}}{\beta_{N_j}\gamma_{N_j}}\right), \tag{2.15}$$

where τ_{N_j} is the lifetime of N_j, β_{N_j} is the velocity in the lab frame, and $\gamma_{N_j} = (1-\beta_{N_j}^2)^{-1/2}$. Though in practice P_{N_j} can be different for two neutrinos, they being degenerate in mass we assume $\Gamma_{N_1} \approx \Gamma_{N_2} = \Gamma_N$, $\beta_{N_1} = \beta_{N_2} \equiv \beta_N$. The effective decay widths including the acceptance factor are

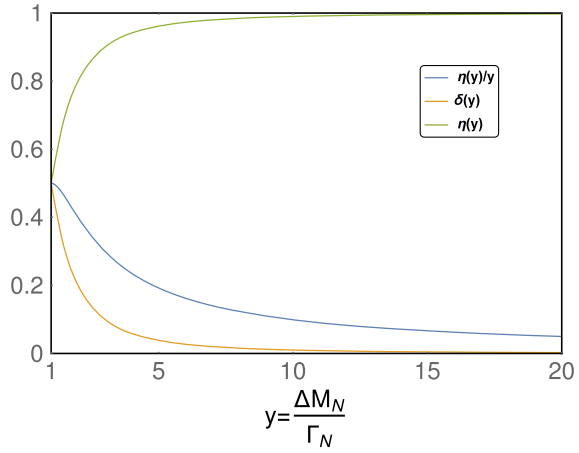

FIG. 2. Variation of overlapping function $\eta(y)$, $\eta(y)/y$, and $\delta(y)$ with $y = \frac{\Delta M_N}{\Gamma_N}$.

$$\Gamma^{\mathrm{LNV(LNC),eff}}_{\mathcal{B}_1/\bar{\mathcal{B}}_1} = \left(1 - \exp\left(-\frac{L\Gamma_N^{\mathrm{M/D}}}{\beta_N\gamma_N}\right)\right)\Gamma^{\mathrm{LNV(LNC)}}_{\mathcal{B}_1/\bar{\mathcal{B}}_1} \tag{2.16}$$

where the expressions of $\Gamma^{\mathrm{LNV(LNC)}}_{\mathcal{B}_1/\bar{\mathcal{B}}_1}$ are given in the previous section, and $\Gamma_N^{\mathrm{M/D}}$ indicate decay rates of Majorana (M) or Dirac (D) neutrinos. For the rest of this section up to the end, we will show the derivations only for the LNV mode. For the LNC mode, only the final expression will be given but the steps of derivations are similar. The effective differential decay width with respect to L for LNV mode is given as

$$\frac{d\Gamma^{\mathrm{LNV,eff}}_{\mathcal{B}_1/\bar{\mathcal{B}}_1}}{dL} = \frac{\Gamma_N^{\mathrm{M}}}{\beta_N\gamma_N}\exp\left(-\frac{L\Gamma_N^{\mathrm{M}}}{\beta_N\gamma_N}\right)\bar{\Gamma}(\mathcal{B}_1 \to \mathcal{B}_2\ell_1^-N)\bar{\Gamma}(N \to \ell_2^-\ell_3^+\nu_{\ell_3}) \times \left\{\frac{|V_{\ell_1N_1}|^2|V_{\ell_2N_1}|^2}{\Gamma_{N_1}^{\mathrm{M}}} + \frac{|V_{\ell_1N_2}|^2|V_{\ell_2N_2}|^2}{\Gamma_{N_2}^{\mathrm{M}}} + \frac{4(|V_{\ell_1N_1}||V_{\ell_2N_1}||V_{\ell_1N_2}||V_{\ell_2N_2}|)}{\Gamma_{N_1}^{\mathrm{M}} + \Gamma_{N_2}^{\mathrm{M}}}\left(\delta(y)\cos(\theta_{21}^{\mathrm{LNV}}) \pm \frac{\eta(y)}{y}\sin(\theta_{21}^{\mathrm{LNV}})\right)\right\}. \tag{2.17}$$

To obtain (2.17) from (2.16) we have used (2.10), (2.11), and (2.12).

We now consider a scenario where the neutrinos are degenerate, i.e., $\Delta M_N \ll m_{N_{i,j}}$, but $\Delta M_N \gg \Gamma_N$. In this case $y \gg 1$ and hence the functions $\delta(y)$ and $\eta(y)/y$ are negligibly small. Physically, this corresponds to a scenario where the overlap between the two neutrinos is negligibly small. In the $y \gg 1$ limit the effective differential decay rates for LNV modes with respect to L are

$$\frac{d\Gamma^{\mathrm{LNV,eff}}_{\mathcal{B}_1/\bar{\mathcal{B}}_1}}{dL} = \frac{\Gamma_N^{\mathrm{M}}}{\beta_N\gamma_N}\exp\left(-\frac{L\Gamma_N^{\mathrm{M}}}{\beta_N\gamma_N}\right)\bar{\Gamma}(\mathcal{B}_1 \to \mathcal{B}_2\ell_1^-N)\bar{\Gamma}(N \to \ell_2^-\ell_3^+\nu_{\ell_3}) \times \left\{\frac{|V_{\ell_1N_1}|^2|V_{\ell_2N_1}|^2}{\Gamma_{N_1}^{\mathrm{M}}} + \frac{|V_{\ell_1N_2}|^2|V_{\ell_2N_2}|^2}{\Gamma_{N_2}^{\mathrm{M}}}\right\}. \tag{2.18}$$

To introduce effects of $N_1 - N_2$ oscillation we note that while a neutrino travels from the production vertex to the decay vertex, it picks up a phase $\exp(-ip_{N_j}\cdot z)$ where p_{N_j} is the four momentum of N_j, $z = (t, 0, 0, L)$ is the space-time separation between the two vertices, and $L \approx \beta_N t$ is the length traveled by the neutrinos between production and decay vertex [84]. This amplitudes is

$$\mathcal{A}^{\rm LNV}_{\rm osc}(\mathcal{B}_1 \to \mathcal{B}_2 \ell_1^- \ell_2^- \ell_3^+ \nu_{\ell_3}; L) \sim V_{\ell_1 N_1} V_{\ell_2 N_1} \exp(-ip_{N_1}\cdot z) + V_{\ell_1 N_2} V_{\ell_2 N_2} \exp(-ip_{N_2}\cdot z). \tag{2.19}$$

The expressions for $\mathcal{A}^{\rm LNV}_{\rm osc}(\bar{\mathcal{B}}_1 \to \bar{\mathcal{B}}_2 \ell_1^+ \ell_2^+ \ell_3^- \bar{\nu}_{\ell_3}; L)$ is obtained by taking complex conjugate of the $V_{\ell N}$ elements in the above formulas. The differential with respect to L of the decay rates that include oscillation effect is proportional to the modulus squared of the amplitudes and we can write

$$\begin{aligned}\frac{d}{dL}\Gamma^{\rm LNV}_{\rm osc}(\mathcal{B}_1 \to \mathcal{B}_2 \ell_1^- \ell_2^- \ell_3^+ \nu_{\ell_3}; L) &\sim |\mathcal{A}^{\rm LNV}_{\rm osc}(\mathcal{B}_1 \to \mathcal{B}_2 \ell_1^- \ell_2^- \ell_3^+ \nu_{\ell_3}; L)|^2 \\ &\sim \sum_{i=1}^{2} |V_{\ell_1 N_i}|^2 |V_{\ell_2 N_i}|^2 \\ &\quad + 2{\rm Re}(V_{\ell_1 N_1} V_{\ell_2 N_1} V^*_{\ell_1 N_2} V^*_{\ell_2 N_2} \exp[i(p_{N_2} - p_{N_1}).z])\end{aligned} \tag{2.20}$$

The superscript "osc" indicates that the oscillation effect is included in the effective differential decay width. Comparing with the differential decay widths (2.18) and (2.20) we get the differential expressions of decay rates that includes oscillation as

$$\frac{d\Gamma^{\rm LNV,osc}_{\mathcal{B}_1/\bar{\mathcal{B}}_1}}{dL} = \frac{\Gamma^{\rm M}_N}{\beta_N \gamma_N} \exp\left(-\frac{L\Gamma^{\rm M}_N}{\beta_N\gamma_N}\right) \bar{\Gamma}(\mathcal{B}_1 \to \mathcal{B}_2 \ell_1^- N) \bar{\Gamma}(N \to \ell_2^- \ell_3^+ \nu_{\ell_3}) \times \left\{ \frac{|V_{\ell_1 N_1}|^2 |V_{\ell_2 N_1}|^2}{\Gamma^{\rm M}_{N_1}} + \frac{|V_{\ell_1 N_2}|^2 |V_{\ell_2 N_2}|^2}{\Gamma^{\rm M}_{N_2}} + \frac{4|V_{\ell_1 N_1}||V_{\ell_2 N_1}||V_{\ell_1 N_2}||V_{\ell_2 N_2}|}{\Gamma^{\rm M}_{N_1} + \Gamma^{\rm M}_{N_2}} \cos\left(\frac{2\pi L}{L_{\rm osc}} \mp \theta^{\rm LNV}_{21}\right) \right\}. \tag{2.21}$$

To simplify the above equations we have used $(p_{N_2} - p_{N_1}).z = 2\pi L/L_{\rm osc}$, and $L_{\rm osc} = 2\pi\beta_N\gamma_N/\Delta M_N = 2\pi\beta_N\gamma_N/(y\Gamma_N)$. Combining (2.17) and (2.21) we get the complete expression of differential decay width that includes both the acceptance factor and the oscillation effects

$$\begin{aligned}\frac{d\Gamma^{\rm LNV,osc}_{\mathcal{B}_1/\bar{\mathcal{B}}_1}}{dL} &= \frac{\Gamma^{\rm M}_N}{\beta_N\gamma_N} \exp\left(-\frac{L\Gamma^{\rm M}_N}{\beta_N\gamma_N}\right) \bar{\Gamma}(\mathcal{B}_1 \to \mathcal{B}_2 \ell_1^- N) \bar{\Gamma}(N \to \ell_2^- \ell_3^+ \nu_{\ell_3}) \\ &\times \left\{ \frac{|V_{\ell_1 N_1}|^2 |V_{\ell_2 N_1}|^2}{\Gamma^{\rm M}_{N_1}} + \frac{|V_{\ell_1 N_2}|^2 |V_{\ell_2 N_2}|^2}{\Gamma^{\rm M}_{N_2}} + \frac{4(|V_{\ell_1 N_1}||V_{\ell_2 N_1}||V_{\ell_1 N_2}||V_{\ell_2 N_2}|)}{\Gamma^{\rm M}_{N_1} + \Gamma^{\rm M}_{N_2}} \left(\delta(y)\cos(\theta^{\rm LNV}_{21}) \pm \frac{\eta(y)}{y}\sin(\theta^{\rm LNV}_{21})\right) \right. \\ &\left. + \frac{4}{\Gamma^{\rm M}_{N_1} + \Gamma^{\rm M}_{N_2}} |V_{\ell_1 N_1}||V_{\ell_2 N_1}||V_{\ell_1 N_2}||V_{\ell_2 N_2}| \cos\left(\frac{2\pi L}{L_{\rm osc}} \mp \theta^{\rm LNV}_{21}\right) \right\},\end{aligned} \tag{2.22}$$

where we have used the Eqs. (2.10)–(2.12). Integrating the above equations with respect to L we obtain

$$\begin{aligned}\Gamma^{\rm LNV,osc}_{\mathcal{B}_1/\bar{\mathcal{B}}_1} \equiv \Gamma(\mathcal{B}_1 \to \mathcal{B}_2 \ell_1^- \ell_2^- \ell_3^+ \nu_{\ell_3}) &= \bar{\Gamma}(\mathcal{B}_1 \to \mathcal{B}_2 \ell_1^- N) \bar{\Gamma}(N \to \ell_2^- \ell_3^+ \nu_{\ell_3}) \left\{ \left[\frac{|V_{\ell_1 N_1}|^2 |V_{\ell_2 N_1}|^2}{\Gamma^{\rm M}_{N_1}} + \frac{|V_{\ell_1 N_2}|^2 |V_{\ell_2 N_2}|^2}{\Gamma^{\rm M}_{N_2}} \right. \right. \\ &+ \frac{4}{\Gamma^{\rm M}_{N_1} + \Gamma^{\rm M}_{N_2}} |V_{\ell_1 N_1}||V_{\ell_2 N_1}||V_{\ell_1 N_2}||V_{\ell_2 N_2}| \left(\delta(y)\cos(\theta^{\rm LNV}_{21}) \pm \frac{\eta(y)}{y}\sin(\theta^{\rm LNV}_{21}) \right) \left. \right] (1 - e^{\frac{-L\Gamma^{\rm M}_N}{\beta_N\gamma_N}}) \\ &+ \frac{4}{\Gamma^{\rm M}_{N_1} + \Gamma^{\rm M}_{N_2}} \frac{1}{1+y^2} |V_{\ell_1 N_1}||V_{\ell_2 N_1}||V_{\ell_1 N_2}||V_{\ell_2 N_2}| \left(e^{\frac{-L\Gamma^{\rm M}_N}{\beta_N\gamma_N}} \left[y \sin\left(\frac{2\pi L}{L_{\rm osc}} \mp \theta^{\rm LNV}_{21}\right) - \cos\left(\frac{2\pi L}{L_{\rm osc}} \mp \theta^{\rm LNV}_{21}\right) \right] \right. \\ &\left. \left. + [\cos(\theta^{\rm LNV}_{21}) \pm y \sin(\theta^{\rm LNV}_{21})] \right) \right\}\end{aligned} \tag{2.23}$$

Following similar steps, we give the final expression for LNC decay

$$\Gamma^{\mathrm{F,LNC,osc}}_{\mathcal{B}_1/\bar{\mathcal{B}}_1} \equiv \Gamma(\mathcal{B}_1 \to \mathcal{B}_2\ell_1^-\ell_2^-\ell_3^+\bar{\nu}_{\ell_2}) = \bar{\Gamma}(\mathcal{B}_1 \to \mathcal{B}_2\ell_1^-N)\bar{\Gamma}(N \to \ell_2^-\ell_3^+\bar{\nu}_{\ell_2})\Bigg\{\Bigg[\frac{|V_{\ell_1N_1}|^2|V_{\ell_3N_1}|^2}{\Gamma^{\mathrm{F}}_{N_1}} + \frac{|V_{\ell_1N_2}|^2|V_{\ell_3N_2}|^2}{\Gamma^{\mathrm{F}}_{N_2}}$$
$$+ \frac{4}{\Gamma^{\mathrm{F}}_{N_1}+\Gamma^{\mathrm{F}}_{N_2}}|V_{\ell_1N_1}||V_{\ell_3N_1}||V_{\ell_1N_2}||V_{\ell_3N_2}|\left(\delta(y)\cos(\theta_{21}^{\mathrm{LNC}}) \pm \frac{\eta(y)}{y}\sin(\theta_{21}^{\mathrm{LNC}})\right)\Bigg](1 - e^{\frac{-L\Gamma^{\mathrm{F}}_N}{\beta_N\gamma_N}})$$
$$+ \frac{4}{\Gamma^{\mathrm{F}}_{N_1}+\Gamma^{\mathrm{F}}_{N_2}}\frac{1}{1+y^2}|V_{\ell_1N_1}||V_{\ell_3N_1}||V_{\ell_1N_2}||V_{\ell_3N_2}|\left(e^{\frac{-L\Gamma^{\mathrm{F}}_N}{\beta_N\gamma_N}}\left[y\sin\left(\frac{2\pi L}{L_{\mathrm{osc}}} \mp \theta_{21}^{\mathrm{LNC}}\right) - \cos\left(\frac{2\pi L}{L_{\mathrm{osc}}} \mp \theta_{21}^{\mathrm{LNC}}\right)\right]\right.$$
$$\left. + [\cos(\theta_{21}^{\mathrm{LNC}}) \pm y\sin(\theta_{21}^{\mathrm{LNC}})]\right)\Bigg\}, \tag{2.24}$$

where F = M (Majorana) or D (Dirac).

III. NUMERICAL ANALYSIS

For numerical analysis, $\Lambda_b^0 \to \Lambda_c^+$ and $\Lambda_b^0 \to p^+$ form factors are taken from the lattice QCD calculations presented in [85]. We leave the decay widths of the sterile neutrinos as phenomenological parameters that can be measured in the experiment. Since the sterile neutrinos are almost degenerate, we will assume their lifetimes to be approximately equal, $\tau_{N_1} \approx \tau_{N_2} = \tau_N$. We present our analysis for $\tau_N = [100, 1000]$ ps [59]. For nearly degenerate neutrinos, it is also natural to assume $|V_{\ell N_1}| \sim |V_{\ell N_2}| \equiv |V_{\ell N}|$. Present experimental bounds on the heavy-to-light mixing are $|V_{eN}|^2 \le 10^{-7}$ and $|V_{\mu N}|^2 \le 10^{-5}$ [36,86]. The neutrinos are expected to travel nearly at the speed of light and we assume that the velocity $\beta_N \ge 0.9$ corresponds to $\beta_N\gamma_N \ge 2$.

The observables of interest are the *CP*-averaged branching ratio and the *CP*-asymmetry. If sterile neutrinos involved are of Majorana types then the final states will include both LNV and LNC states and the *CP*-averaged branching ratio is

$$\mathcal{B}r^{\mathrm{M}} \approx \frac{1}{2}(\mathcal{B}r^{\mathrm{M,LNC,osc}}_{\mathcal{B}_1} + \mathcal{B}r^{\mathrm{M,LNV,osc}}_{\mathcal{B}_1} + \mathcal{B}r^{\mathrm{M,LNC,osc}}_{\bar{\mathcal{B}}_1} + \mathcal{B}r^{\mathrm{M,LNV,osc}}_{\bar{\mathcal{B}}_1}). \tag{3.1}$$

The branching ratios are obtained from decay rates by dividing with the total decay rates of $\mathcal{B}_1$ baryons. For simplicity, we have assumed that $\mathcal{B}_1$ and $\bar{\mathcal{B}}_1$ have the same decay rates and that is why we have used $\approx$ in the above equation. The *CP*-asymmetry observable for Majorana induced decay is

$$\mathcal{A}^{\mathrm{M}}_{CP} = \frac{(\Gamma^{\mathrm{M,LNC,osc}}_{\mathcal{B}_1} + \Gamma^{\mathrm{M,LNV,osc}}_{\mathcal{B}_1}) - (\Gamma^{\mathrm{M,LNC,osc}}_{\bar{\mathcal{B}}_1} + \Gamma^{\mathrm{M,LNV,osc}}_{\bar{\mathcal{B}}_1})}{(\Gamma^{\mathrm{M,LNC,osc}}_{\mathcal{B}_1} + \Gamma^{\mathrm{M,LNV,osc}}_{\mathcal{B}_1}) + (\Gamma^{\mathrm{M,LNC,osc}}_{\bar{\mathcal{B}}_1} + \Gamma^{\mathrm{M,LNV,osc}}_{\bar{\mathcal{B}}_1})}. \tag{3.2}$$

When Dirac neutrino is involved then there are only LNC final states and *CP*-averaged branching ratio and the *CP*-asymmetry are defined as

$$\mathcal{B}r^{\mathrm{D}} \approx \frac{1}{2}(\mathcal{B}r^{\mathrm{D,LNC,osc}}_{\mathcal{B}_1} + \mathcal{B}r^{\mathrm{D,LNC,osc}}_{\bar{\mathcal{B}}_1}),$$
$$\mathcal{A}^{\mathrm{D}}_{CP} = \frac{(\Gamma^{\mathrm{D,LNC,osc}}_{\mathcal{B}_1} - \Gamma^{\mathrm{D,LNC,osc}}_{\bar{\mathcal{B}}_1})}{(\Gamma^{\mathrm{D,LNC,osc}}_{\mathcal{B}_1} + \Gamma^{\mathrm{D,LNC,osc}}_{\bar{\mathcal{B}}_1})}. \tag{3.3}$$

We first consider decays occurring through a Majorana neutrino in the intermediate state so that there are both LNV and LNC final states. In Fig. 3 we show the *CP*-averaged branching ratios for $\Lambda_b^0 \to (\Lambda, p)\mu\mu e\nu$ as a function of neutrino mass m_{N_1}. For simplicity we chose $\theta_{21}^{\mathrm{LNV}} = \theta_{21}^{\mathrm{LNC}}$ though in general the *CP*-odd pases can be different. The plots are obtained for neutrino displaced vertex length $L = 100$ cm, $\gamma_N\beta_N = 2$, $\tau_N = 100$ ps, and the mass difference is $\Delta M_N = 5 \times 10^{-14}$ GeV. Maximum branching ratios are obtained at $m_{N_1} = 2$ GeV for $\Lambda_b^0 \to \Lambda_c\mu\mu e\nu$ and at $m_{N_1} = 3.2$ GeV for $\Lambda_b^0 \to p\mu\mu e\nu$ modes. In Fig. 4, for $\tau_N = 100$, 1000 ps we show the *CP*-averaged branching ratios for $\Lambda_b^0 \to (\Lambda_c, p)\mu\mu e\nu$ for different values of $\gamma_N\beta_N$ and for fixed values of $\theta_{21}^{\mathrm{LNV}}$ and $\theta_{21}^{\mathrm{LNC}}$. From the figures we find the *CP*-averaged branching ratios of $\Lambda_b^0 \to \Lambda_c\mu\mu e\nu$ lie between 10^{-10}–10^{-9}, whereas branching ratios for $\Lambda_b^0 \to p\mu\mu e\nu$ lie between 10^{-11}–10^{-10}. The one order of magnitude suppression in the $\Lambda_b^0 \to p\mu\mu e\nu$ mode with respect to the $\Lambda_b^0 \to \Lambda\mu\mu e\nu$ is attributed to Cabibbo-Kobayashi-Maskawa matrix elements. We find that the branching ratios for $\Lambda_b^0 \to (\Lambda_c, p)ee\mu\nu$ are one orders of magnitude suppressed compared to $\Lambda_b^0 \to (\Lambda_c, p)\mu\mu e\nu$ but the qualitative features are same as seen in Figs. 3 and 4. Though LNV and LNC both are present in case of Majorana induced decay, LNV modes dominate over the LNC modes in the case of $\Lambda_b^0 \to (\Lambda_c, p)\mu\mu e\nu$ but for the decay mode $\Lambda_b^0 \to (\Lambda_c, p)ee\mu\nu$, LNC decays dominate over LNV. This can be explained as follows: In $\Lambda_b^0 \to (\Lambda_c, p)\mu\mu e\nu$ decays the LNV modes are proportional to $|V_{\mu N}|^4 \sim 10^{-10}$ where as the LNC branching ratios are proportional to $|V_{\mu N}|^2|V_{eN}|^2 \sim 10^{-12}$. In $\Lambda_b^0 \to (\Lambda_c, p)ee\mu\nu$ decays the LNV modes are proportional to $|V_{eN}|^4 \sim 10^{-14}$ and the LNC modes are proportional to $|V_{\mu N}|^2|V_{eN}|^2 \sim 10^{-12}$.

To compare branching ratios mediated by Dirac neutrinos, in Fig. 5 we show the *CP* averaged branching ratios

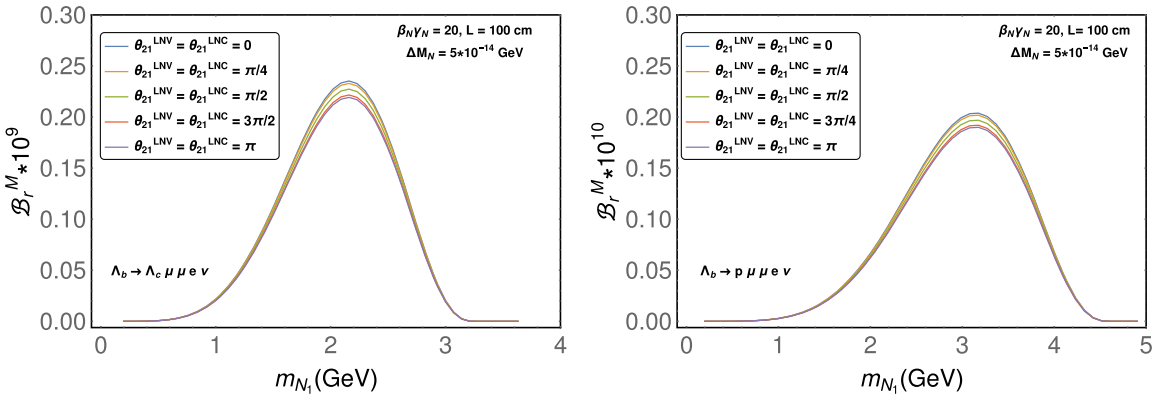

FIG. 3. Branching ratios $\mathcal{B}r^{\mathrm{M}}(\Lambda_b^0 \to \Lambda_c \mu\mu e\nu)$ and $\mathcal{B}r^{\mathrm{M}}(\Lambda_b^0 \to p\mu\mu e\nu)$ as a function of m_{N_1} for $|V_{\mu N_1}|^2 = |V_{\mu N_2}|^2 = 10^{-5}$, $|V_{eN_1}|^2 = |V_{eN_2}|^2 = 10^{-7}$, $\Delta M_N = 5 \times 10^{-14}$ GeV, $\beta_N\gamma_N = 20$, maximal displaced vertex length $L = 100$ cm, $\tau_{N_1} = \tau_{N_2} = 100$ ps, and for different values of weak phase angles $\theta_{21}^{\mathrm{LNV}}$ and $\theta_{21}^{\mathrm{LNC}}$.

for $\Lambda_b^0 \to (\Lambda, p)\mu\mu e\nu$ as a function of m_{N_1}. The plots are shown for $\tau_N = 100$ ps where as the rest of the parameter choices are same as in Fig. 4. Similar plots are obtained for $\mathcal{B}r(\Lambda_b^0 \to (\Lambda, p)ee\mu\nu)$ modes. Qualitatively, the plots are similar to what we obtained for these modes with Majorana neutrinos. For the Dirac case, we get the similar plot like Fig. 3 but there are two order suppression of magnitude. Quantitatively, $\mathcal{B}r^{\mathrm{D}}(\Lambda_b^0 \to (\Lambda_c, p)\mu\mu e\nu)$ is two orders of magnitude smaller than $\mathcal{B}r^{\mathrm{M}}(\Lambda_b^0 \to (\Lambda_c, p)\mu\mu e\nu)$ where as $\mathcal{B}r^{\mathrm{M}}(\Lambda_b^0 \to (\Lambda_c, p)ee\mu\nu)$ and $\mathcal{B}r^{\mathrm{D}}(\Lambda_b^0 \to (\Lambda_c, p)ee\mu\nu)$ are of the same order of magnitude.

In Fig. 6 we show the CP-averaged branching ratios as a function of maximal displaced vertex length L for decays involving Majorana neutrinos. The Majorana neutrino mass

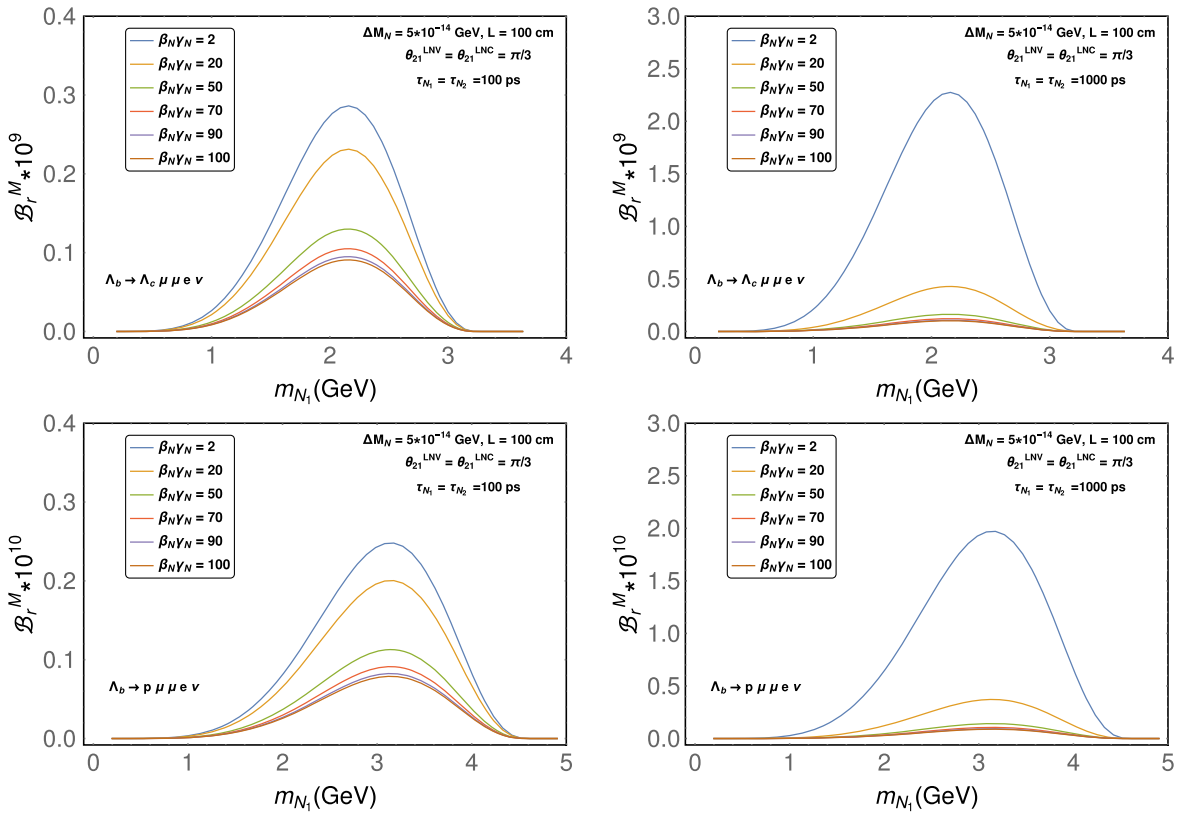

FIG. 4. Branching ratios $\mathcal{B}r^{\mathrm{M}}(\Lambda_b^0 \to (\Lambda_c, p)\mu\mu e\nu)$ as a function of m_{N_1} for the values of heavy light mixing elements $|V_{\mu N_1}|^2 = |V_{\mu N_2}|^2 = 10^{-5}$, $|V_{eN_1}|^2 = |V_{eN_2}|^2 = 10^{-7}$ and $\Delta M_N = 5 \times 10^{-14}$ GeV, weak phase angles $\theta_{21}^{\mathrm{LNV}} = \theta_{21}^{\mathrm{LNC}} = \pi/3$, neutrino flight length $L = 100$ cm and $\tau_{N_1} = \tau_{N_2} = [100, 1000]$ ps for different values of Lorentz factors $\beta_N\gamma_N$.

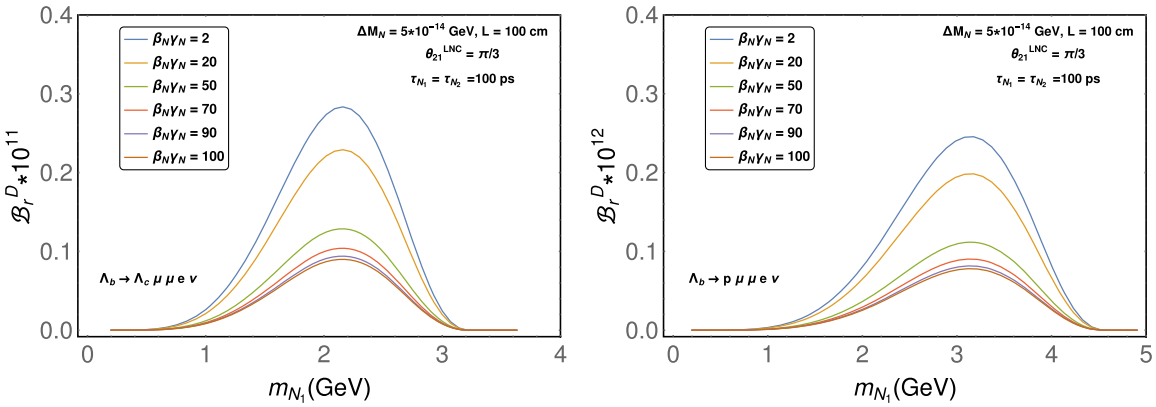

FIG. 5. *CP* average branching ratios $\mathcal{B}r^{\mathrm{D}}(\Lambda_b^0 \to (\Lambda_c, p)\mu\mu e\nu)$ mediated by Dirac neutrinos as a function of m_{N_1} for the values of heavy light mixing elements $|V_{\mu N_1}|^2 = |V_{\mu N_2}|^2 = 10^{-5}$, $|V_{eN_1}|^2 = |V_{eN_2}|^2 = 10^{-7}$ and $\Delta M_N = 5 \times 10^{-14}$ GeV, weak phase angles $\theta_{21}^{\mathrm{LNC}} = \pi/3$, neutrino flight length $L = 100$ cm and $\tau_{N_1} = \tau_{N_2} = 100$ ps for different values of Lorentz factors $\beta_N\gamma_N$.

$m_{N_1} = 2$ GeV for $\Lambda_b^0 \to \Lambda_c\mu\mu e\nu$ and $m_{N_1} = 3.2$ GeV for $\Lambda_b^0 \to p\mu\mu e\nu$ and the values of the rest of the parameters are shown in the legends of the plots. The troughs and crests are modulations resulting from the oscillation effect that is clearly visible from these plots. These plots indicate that for sufficiently small detector length $L_{\mathrm{det}} < L$, a significant fraction of neutrinos will decay outside the detector leading to a small branching ratio. For $L_{\mathrm{det}} > L$, most neutrinos decay inside, and therefore the branching ratio saturates. From the Fig. 6, we also observe that saturation in L can happen early for a small value of $\gamma_N\beta_N$. As we notice from the Eq. (2.15), the acceptance factor is larger for the lower value of $\gamma_N\beta_N$.

In the left panel of Fig. 7 we show *CP*-asymmetry observable $\mathcal{A}_{CP}$ for $\Lambda_b^0 \to \Lambda_c\mu\mu e\nu$ as a function of y for different values of $\theta_{21}^{\mathrm{LNV}}$ and $\theta_{21}^{\mathrm{LNC}}$ and $L = 100$ cm. This

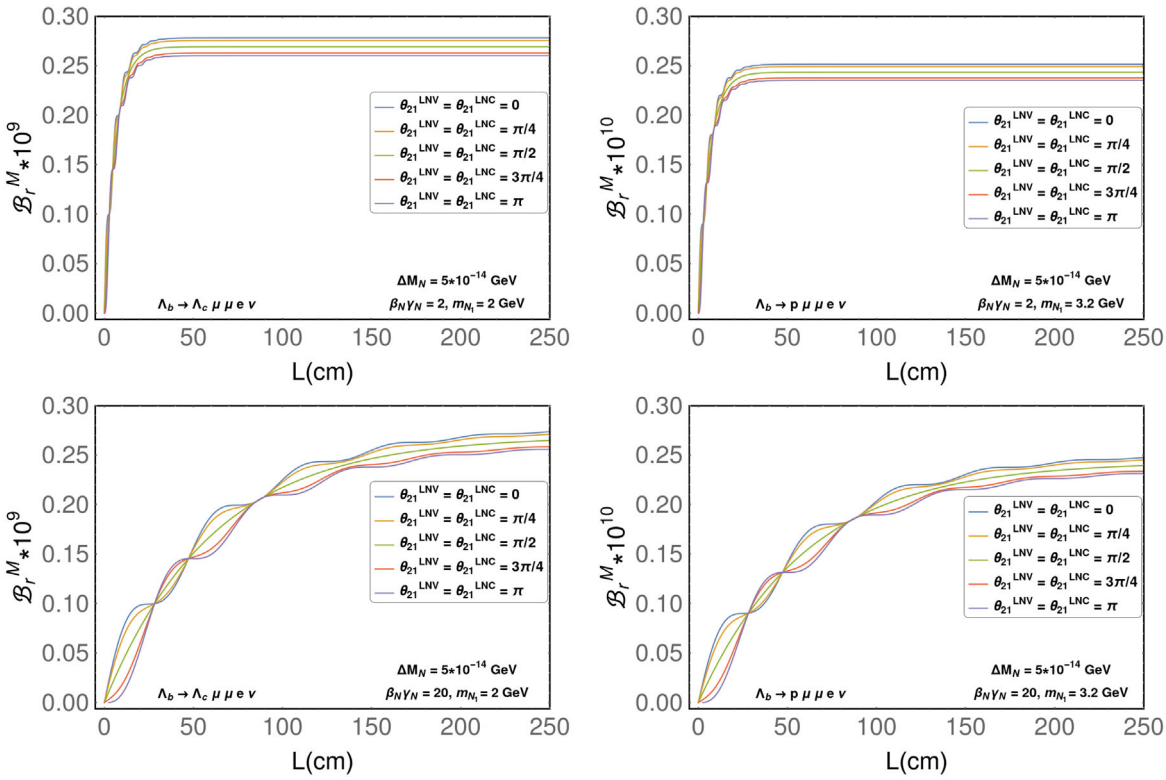

FIG. 6. Branching ratios $\mathcal{B}r^{\mathrm{M}}(\Lambda_b^0 \to (\Lambda_c, p)\mu\mu e\nu)$ as a function of the neutrino flight length L in cm for different values of weak phase angles $\theta_{21}^{\mathrm{LNV}}$, $\theta_{21}^{\mathrm{LNC}}$ and for the values of heavy light mixing $|V_{\mu N_1}|^2 = |V_{\mu N_2}|^2 = 10^{-5}$, $|V_{eN_1}|^2 = |V_{eN_2}|^2 = 10^{-7}$ and mass difference $\Delta M_N = 5 \times 10^{-14}$ GeV, Lorentz factors $\beta_N\gamma_N = [2, 20]$, Majorana mass $M_{N_1} = 2$ GeV and 3.2 GeV for Λ_c and proton receptively, $\tau_{N_1} = \tau_{N_2} = 100$ ps.

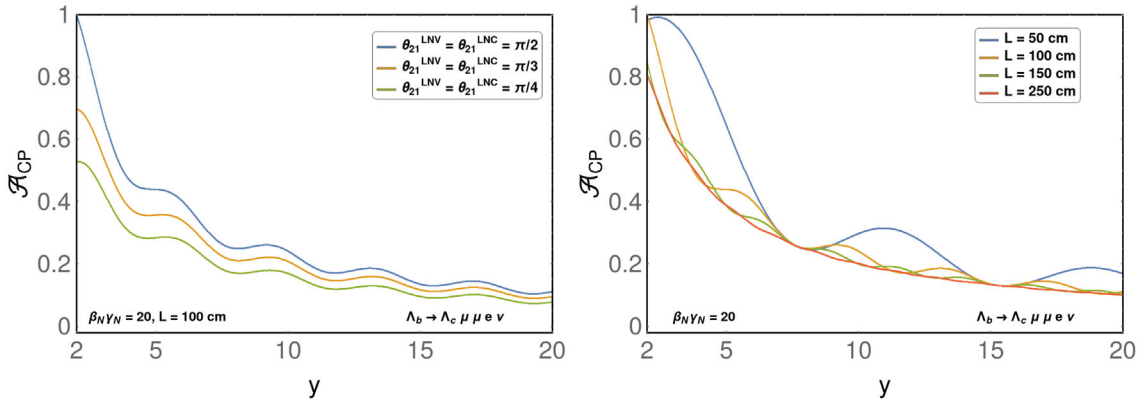

FIG. 7. The CP asymmetry observable $\mathcal{A}_{CP}$ for $\Lambda_b^0 \to \Lambda_c \mu\mu e\nu$ as a function of $y = \frac{\Delta M_N}{\Gamma_N}$ for different values of phases (left panel) and maximal decay vertex (right panel) and for the values of $|V_{\mu N_1}|^2 = |V_{\mu N_2}|^2 = 10^{-5}$, $|V_{eN_1}|^2 = |V_{eN_2}|^2 = 10^{-7}$ and $\tau_N = 100$ ps. Similar plots are obtained for $\Lambda_b^0 \to p\mu\mu e\nu$ and $\Lambda_b^0 \to (\Lambda_c, p)ee\mu\nu$.

plot demonstrates that the maximum value of CP-asymmetry is obtained when the CP-odd phases are $\pi/2$. From the left panel of Fig. 7, it is also seen that $\mathcal{A}_{CP}$ gradually decreases with increasing y because the overlap between the two neutrinos decreases. In the right panel of Fig. 7 we show $\mathcal{A}_{CP}$ with respect to y for different values of maximal neutrino displaced vertex length L, CP-odd phases $\theta_{21}^{\rm LNV} = \theta_{21}^{\rm LNC} = \pi/2$, $\tau_N = 100$ ps, and $\gamma_N\beta_N = 20$. We observe that the maximum value of $\mathcal{A}_{CP}$ is obtained for $y < 8$. A strong dependence of $\mathcal{A}_{CP}$ on maximum displaced vertex length L is also observed. For large values of L the modulation is suppressed as can be seen from (2.23) and (2.24). In Fig. 8, for the different values of y, we show the variation of $\mathcal{A}_{CP}$ with respect to L. The left and the right panels are for $\gamma_N\beta_N = 20$ and $\gamma_N\beta_N = 50$, respectively. This means that oscillations length is lower in the left plot. It is again observed that the maximum value of $\mathcal{A}_{\rm CP}$ is observed when maximal displaced vertex L is comparable to $L_{\rm osc}$. For large L, the modulations are suppressed by the exponential term as can be seen from Eqs. (2.23) and (2.24).

Similar plots are also obtained for Majorana neutrino mediated $\Lambda_b^0 \to p\mu\mu e\nu$ and $\Lambda_b^0 \to (\Lambda_c, p)ee\mu\nu$ decays. We reach similar conclusions when decays are due to Dirac neutrinos.

Even if the decay modes are not observed, upper limits on the branching ratios can be translated to constraints on the heavy-to-light mixing elements. For example, if upper limits on branching ratios $\mathcal{B}r^{\rm M}(\Lambda_b^0 \to \Lambda_c\mu\mu e\nu) < 10^{-7}, 10^{-8}$ and $\mathcal{B}r^{\rm M}(\Lambda_b^0 \to p\mu\mu e\nu) < 10^{-8}, 10^{-9}$ is reported, then it can be translated to constraints on the $(m_{N_1}, |V_{\mu N}|^2)$ plane as shown in Fig. 9. To obtain this plot, we have neglected the LNC contributions for simplicity as it is two orders of magnitude suppressed. The light and dark shaded regions represent the exclusion regions correspond for $\tau_{N_1} = \tau_{N_2} =$ 100 ps and 1000 ps respectively. To compare our bounds with experimental results, we have superimposed in Fig. 9, the exclusion limits coming from different experiments like LHCb [33,77], Belle [87], L3 [88], Delphi [89], NA3 [90], CHARM [91], NuTeV [92] and NA48 [78]. In Fig. 10 we

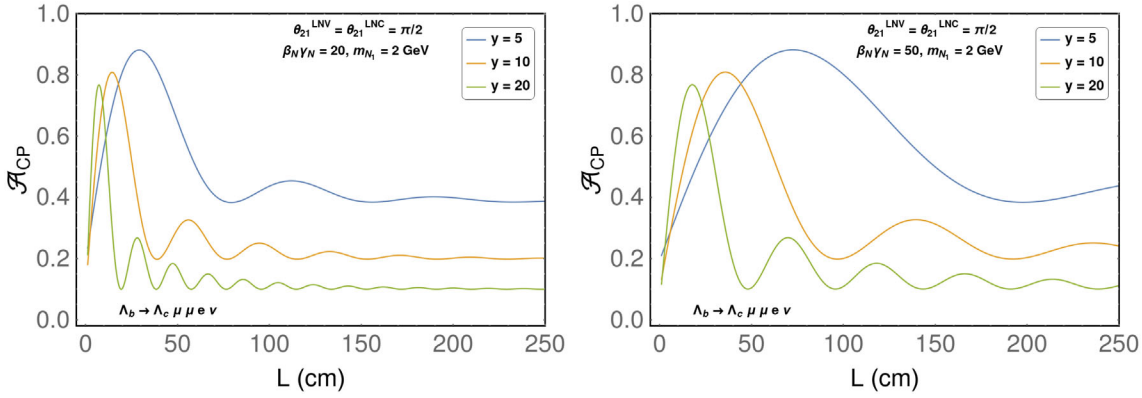

FIG. 8. The CP asymmetry observable $\mathcal{A}_{CP}$ as a function of displaced vertex length L for the decay mode $\Lambda_b^0 \to \Lambda_c\mu\mu e\nu$ for different values of $y = \frac{\Delta M_N}{\Gamma_N}$ and for the values of $|V_{\mu N_1}|^2 = |V_{\mu N_2}|^2 = 10^{-5}$, $|V_{eN_1}|^2 = |V_{eN_2}|^2 = 10^{-7}$, $M_{N1} = 2$ GeV, $\theta_{21}^{\rm LNV} = \theta_{21}^{\rm LNC} = \pi/2$, $\beta_N\gamma_N = 20$, $\tau_{N_1} = \tau_{N_2} = 100$ ps. An identical plots are obtained for $\Lambda_b^0 \to p\mu\mu e\nu$ and $\Lambda_b^0 \to (\Lambda_c, p)ee\mu\nu$.

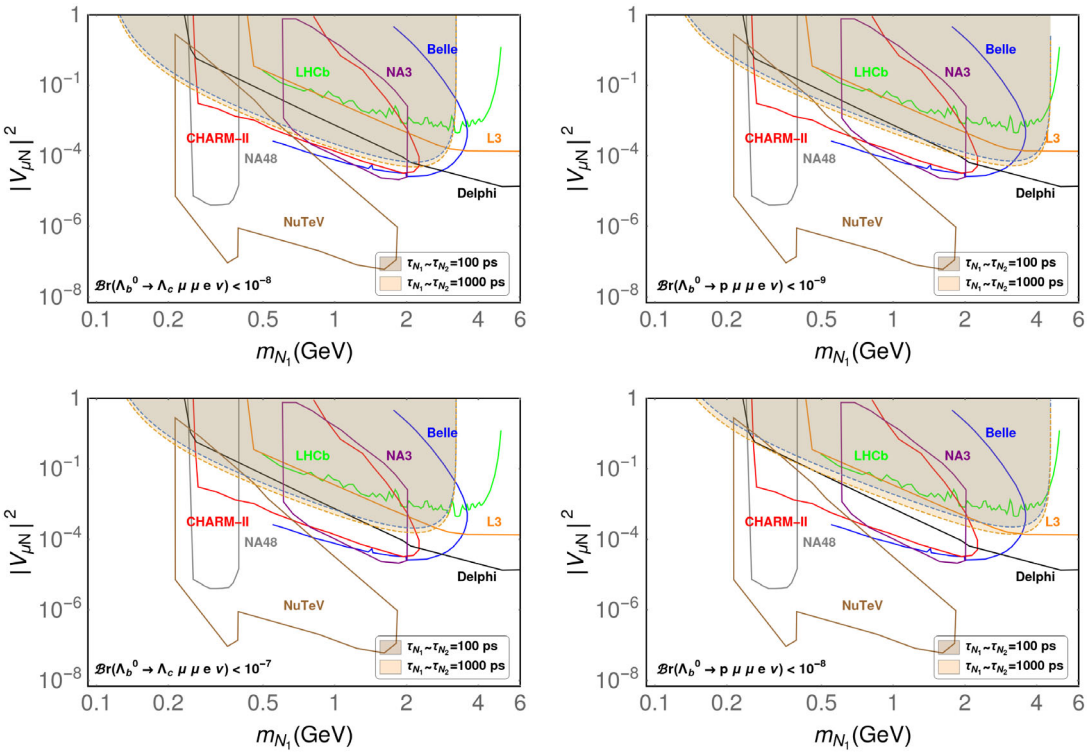

FIG. 9. Exclusion regions on the $(|V_{\mu N}|^2, m_{N_1})$ parameter space for the case of LNV decays mediated by Majorana neutrinos for $\mathcal{B}r^{\mathrm{M}}(\Lambda_b^0 \to p\mu\mu e\nu) < 10^{-8}, 10^{-9}$ and $\mathcal{B}r^{\mathrm{M}}(\Lambda_b^0 \to \Lambda_c\mu\mu e\nu) < 10^{-7}, 10^{-8}$ for the values of $\tau_{N_1} = \tau_{N_2} = [100, 1000]$ ps, $\theta_{21}^{\mathrm{LNV}} = \pi/3$, $\Delta M_N = 5 \times 10^{-14}$ GeV, $\beta_N\gamma_N = 20$ and $L = 100$ cm.

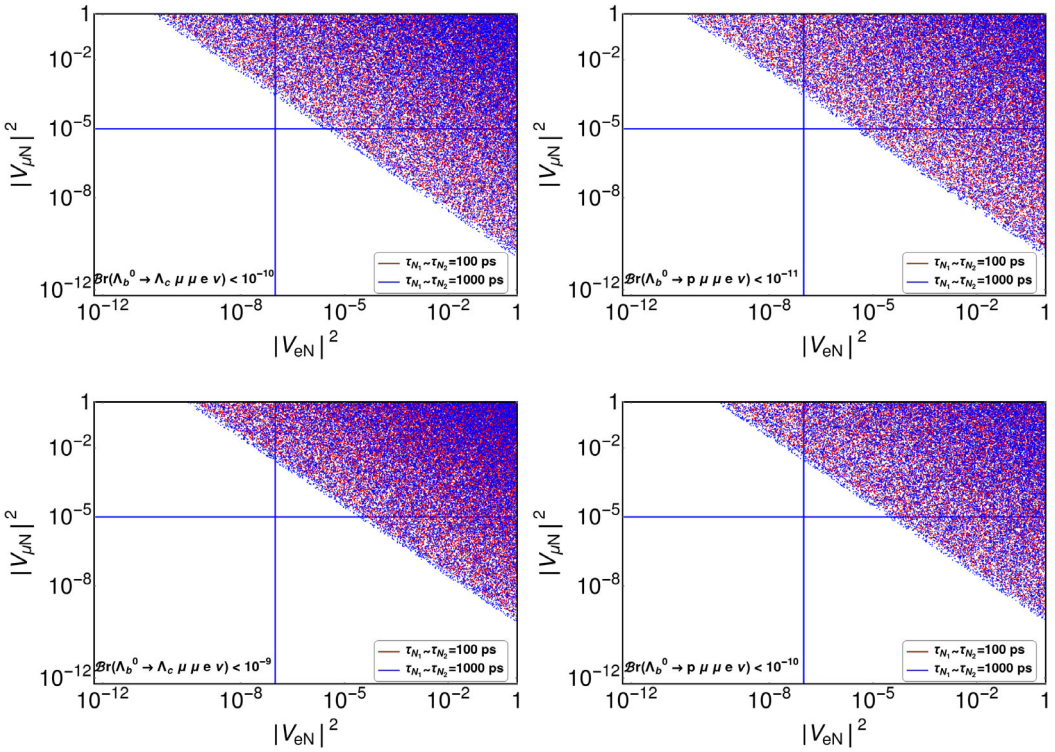

FIG. 10. Exclusion regions on the $(|V_{eN}|^2, |V_{\mu N}|^2)$ parameter space for the case of LNC decays mediated by Dirac neutrinos for $\mathcal{B}r^{\mathrm{D}}(\Lambda_b^0 \to p\mu\mu e\nu) < 10^{-10}, 10^{-11}$ and $\mathcal{B}r^{\mathrm{D}}(\Lambda_b^0 \to \Lambda_c\mu\mu e\nu) < 10^{-9}, 10^{-10}$ for the fixed values of $\tau_{N_1} = \tau_{N_2} = [100, 1000]$ ps, $\theta_{21}^{\mathrm{LNV}} = \pi/3$, $\Delta M_N = 5 \times 10^{-14}$ GeV, $\beta_N\gamma_N = 20$, $L = 100$ cm, and $m_{N_1} = 2$ GeV and 3.2 GeV for Λ_c and proton respectively. Vertical and horizontal lines correspond to the present upper bounds on heavy-to-light mixing elements.

show the constraints on the $(|V_{eN}|^2, |V_{\mu N}|^2)$ parameter space for $\mathcal{B}r^{\mathrm{D}}(\Lambda_b^0 \to \Lambda_c \mu\mu e\nu) < 10^{-9}, 10^{-10}$ and $\mathcal{B}r^{\mathrm{D}}(\Lambda_b^0 \to p\mu\mu e\nu) < 10^{-10}, 10^{-11}$. Here the mass of the Dirac neutrino $m_{N_1} = 2$ GeV and 3.2 GeV for Λ_c and p respectively and the mass difference $\Delta M_N = 5 \times 10^{-14}$ GeV for both cases. The rest of the parameters are mentioned in the caption of the plots. The vertical and horizontal lines correspond to the present upper bounds on the heavy to light mixing elements.

At the LHC, about 5% of total b-hadrons formed are Λ_b^0. The LHCb is already capable of studying rare decays of Λ_b^0 and has already observed $\Lambda_b^0 \to \Lambda\mu^+\mu^-$ [93,94]. The decay modes discussed in this paper may be within the reach of future LHCb. Even if the modes are not seen, the upper limits can still be translated to complementary bounds on the heavy-to-light mixing elements $|V_{\ell N}|^2$.

IV. SUMMARY

In this paper we have studied $\Lambda_b^0 \to (\Lambda_c^+, p^+)\ell_1^-\ell_2^-\ell_3^+\nu$ and its conjugate decays mediated by two quasi-degenerate GeV-scale sterile neutrinos. Both Majorana and Dirac neutrinos have been considered and we have focused on kinematical regions where the neutrinos can be on-shell. The heavy neutrino acceptance factor and effects of oscillations are included in the decay rates. We find that the CP-averaged branching ratio for $\Lambda_b^0 \to p\ell_1\ell_2\ell_3\nu$ is one orders of magnitude suppressed compared to $\Lambda_b^0 \to \Lambda_c\ell_1\ell_2\ell_3\nu$ due to Cabbibo-Kobayashi-Maskawa suppression. For the $\Lambda_b^0 \to (\Lambda_c, p)\mu\mu e\nu$ mode, the Majorana induced transition is two orders of magnitude larger than the Dirac induced transition. For the $\Lambda_b^0 \to (\Lambda_c, p)ee\mu\nu$ mode, the branching ratios for Majorana and Dirac induced transitions are of the same order of magnitude. Numerically, we have explored the possibility of CP-violation and find that it is appreciable when the neutrino mass difference is of the order of their average decay widths.

ACKNOWLEDGMENTS

D. D. acknowledges the DST, Government of India for the INSPIRE Faculty Fellowship (Grant No. IFA16-PH170). J. D. acknowledges the Council of Scientific and Industrial Research (CSIR), Government of India for SRF fellowship grant with File No. 09/045(1511)/2017-EMR-I.

APPENDIX A: FIVE-BODY DECAYS OF $\mathcal{B}_1(p)(\to \mathcal{B}_2(k)\ell_1(p_1)\ell_2^-(p_2)\ell_3^+(p_3)\nu(p_\nu))$

The decays proceeds in two steps, $\mathcal{B}_1(b) \to \mathcal{B}_2(c/u)\ell_1^- N_j$ followed by the decay of the neutrinos $N_j \to \ell_2^-\ell_3^+\nu$. The direct ($D$) or a crossed ($C$) channel as shown in Fig. 1. For jth neutrino in the intermediate state, we can write the matrix elements for D and C channels as

$$\begin{aligned}
\mathcal{M}_{D_j}^{\mathrm{LNV}\pm} &= (G_F^2 V_{bq}^{(*)} m_{N_j})(v_{X_i}^{\mathrm{LNV},\pm}) P_{D_j}^{\mathrm{LNV}} H_\nu^\pm L_{\mathrm{LNV,D}}^{\nu\alpha\pm} l_{\mathrm{X},\alpha}^{\mathrm{LNV}\pm} \\
\mathcal{M}_{C_j}^{\mathrm{LNV}\pm} &= (G_F^2 V_{bq}^{(*)} m_{N_j})(v_{X_i}^{\mathrm{LNV},\pm}) P_{C_j}^{\mathrm{LNV}} H_\nu^\pm L_{\mathrm{LNV,C}}^{\alpha\nu\pm} l_{\mathrm{X},\alpha}^{\mathrm{LNV}\pm} \\
\mathcal{M}_{D_j}^{\mathrm{LNC}\pm} &= (G_F^2 V_{bq}^{(*)} m_{N_j})(v_{D_i}^{\mathrm{LNC},\pm}) P_{D_j}^{\mathrm{LNC}} H_\nu^\pm L_{\mathrm{LNC,D}}^{\nu\alpha\pm} l_{\mathrm{D},\alpha}^{\mathrm{LNC}\pm} \\
\mathcal{M}_{C_j}^{\mathrm{LNC}\pm} &= (G_F^2 V_{bq}^{(*)} m_{N_j})(v_{C_i}^{\mathrm{LNC},\pm}) P_{C_j}^{\mathrm{LNC}} H_\nu^\pm L_{\mathrm{LNC,C}}^{\alpha\nu\pm} l_{\mathrm{C},\alpha}^{\mathrm{LNC}\pm}
\end{aligned} \tag{A1}$$

Here the superscripts "+" and "−" are for $\mathcal{B}_1(b) \to \mathcal{B}_2(q)\ell_1^-\ell_2^-\ell_3^+\nu$ and its CP-conjugate mode $\bar{\mathcal{B}}_1(\bar{b}) \to \bar{\mathcal{B}}_2(\bar{q})\ell_1^+\ell_2^+\ell_3^-\bar{\nu}$ respectively. The heavy to light mixing elements $v_{X_i}^{Z,\pm}$ (Z = LNV or LNC) are given in following.

$$\begin{aligned}
&v_{D_i}^{\mathrm{LNC},+} = V_{\ell_1 N_i}(V_{\ell_3 N_i})^*, \qquad v_{C_i}^{\mathrm{LNC},+} = V_{\ell_2 N_i}(V_{\ell_3 N_i})^*, \\
&v_{X_i}^{\mathrm{LNC},-} = (v_{X_i}^{\mathrm{LNC},+})^* \\
&v_{D_i}^{\mathrm{LNV},+} = v_{C_i}^{\mathrm{LNV},+} = v_{X_i}^{\mathrm{LNV},+} = V_{\ell_1 N_i} V_{\ell_2 N_i}, \\
&v_{X_i}^{\mathrm{LNV},-} = (v_{X_i}^{\mathrm{LNV},+})^*, \quad X = C, D
\end{aligned} \tag{A2}$$

The leptonic part of the amplitudes are

$$\begin{aligned}
L_{\mathrm{LNV,D}}^{\nu\alpha+} &= \bar{u}_{\ell_1}(p_1)\gamma^\nu\gamma^\alpha(1+\gamma_5)v_{\ell_2}(p_2), & L_{\mathrm{LNV,D}}^{\nu\alpha-} &= \bar{v}_{\ell_2}(p_2)\gamma^\alpha\gamma^\nu(1-\gamma_5)u_{\ell_1}(p_1) \\
L_{\mathrm{LNV,C}}^{\alpha\nu+} &= \bar{u}_{\ell_1}(p_1)\gamma^\alpha\gamma^\nu(1+\gamma_5)v_{\ell_2}(p_2), & L_{\mathrm{LNV,C}}^{\alpha\nu-} &= \bar{v}_{\ell_2}(p_2)\gamma^\nu\gamma^\alpha(1-\gamma_5)u_{\ell_1}(p_1) \\
L_{\mathrm{LNC,D}}^{\nu\alpha+} &= \bar{u}_{\ell_1}(p_1)\gamma^\nu \not{k}_N \gamma^\alpha(1-\gamma_5)v_{\ell_3}(p_3), & L_{\mathrm{LNC,D}}^{\nu\alpha-} &= \bar{v}_{\ell_3}(p_3)\gamma^\alpha \not{k}_N \gamma^\nu(1-\gamma_5)u_{\ell_1}(p_1) \\
L_{\mathrm{LNC,C}}^{\alpha\nu+} &= \bar{u}_{\ell_1}(p_2)\gamma^\nu \not{k}_N \gamma^\alpha(1-\gamma_5)v_{\ell_3}(p_3), & L_{\mathrm{LNC,C}}^{\alpha\nu-} &= \bar{v}_{\ell_3}(p_3)\gamma^\alpha \not{k}_N \gamma^\nu(1-\gamma_5)u_{\ell_1}(p_2).
\end{aligned} \tag{A3}$$

Using the lattice QCD parametrizations of the form factors given in [85] we get the expression of the hadronic amplitude as

$$\begin{aligned}
H^\mu &= \langle \mathcal{B}_2(k, s_k)|\bar{c}\gamma^\mu(1-\gamma_5)b|\mathcal{B}_1(p, s_p)\rangle \\
&= \bar{u}(k, s_k)(A_1 q^\mu + A_2 k^\mu + A_3\gamma^\mu + \gamma_5\{A_4 q^\mu + A_5 k^\mu + A_6\gamma^\mu\})u(p, s_p).
\end{aligned} \tag{A4}$$

where we have used $p = q + k$ we can even write where the q^2 dependent functions are given as

$$
\begin{aligned}
A_1 &= f_t^V \frac{m_{\mathcal{B}1} - m_{\mathcal{B}2}}{q^2} + f_0^V \frac{m_{\mathcal{B}1} + m_{\mathcal{B}2}}{s_+}\left(1 - \frac{m_{\mathcal{B}_1}^2 - m_{\mathcal{B}_2}^2}{q^2}\right) - f_\perp^V \frac{2m_{\mathcal{B}2}}{s_+},\\
A_2 &= 2f_0^V \frac{m_{\mathcal{B}1} + m_{\mathcal{B}2}}{s_+} - f_\perp^V\left(\frac{2m_{\mathcal{B}2}}{s_+} + \frac{2m_{\mathcal{B}1}}{s_+}\right),\\
A_3 &= f_\perp^V,\\
A_4 &= f_t^A \frac{m_{\mathcal{B}1} + m_{\mathcal{B}2}}{q^2} + f_0^A \frac{m_{\mathcal{B}1} - m_{\mathcal{B}2}}{s_-}\left(1 - \frac{m_{\mathcal{B}_1}^2 - m_{\mathcal{B}_2}^2}{q^2}\right) + f_\perp^A \frac{2m_{\mathcal{B}2}}{s_-},\\
A_5 &= 2f_0^A \frac{m_{\mathcal{B}1} - m_{\mathcal{B}2}}{s_-} + f_\perp^A\left(\frac{2m_{\mathcal{B}2}}{s_-} - \frac{2m_{\mathcal{B}1}}{s_-}\right),\\
A_6 &= f_\perp^A.
\end{aligned}
\tag{A5}
$$

With reference to Fig. 1 the decay of the W^+ and W^- for LNV and LNC processes respectively proceeds through the following currents

$$
\begin{aligned}
l_{\mathrm{X},\alpha}^{\mathrm{LNV}+} &= \bar{u}_{\nu_{\ell_3}}\gamma_\alpha(1-\gamma_5)v_{\ell_3}, \qquad l_{\mathrm{X},\alpha}^{\mathrm{LNV}-} = \bar{u}_{\ell_3}\gamma_\alpha(1-\gamma_5)v_{\bar{\nu}_{\ell_3}} = (l_{\mathrm{X},\alpha}^{\mathrm{LNV},+})^\dagger\\
l_{\mathrm{D},\alpha}^{\mathrm{LNC}+} &= \bar{u}_{\ell_2}\gamma_\alpha(1-\gamma_5)v_{\bar{\nu}_{\ell_2}}, \qquad l_{\mathrm{D},\alpha}^{\mathrm{LNC}-} = \bar{u}_{\nu_{\ell_2}}\gamma_\alpha(1-\gamma_5)v_{\ell_2} = (l_{\mathrm{D},\alpha}^{\mathrm{LNC},+})^\dagger\\
l_{\mathrm{C},\alpha}^{\mathrm{LNC}+} &= \bar{u}_{\ell_1}\gamma_\alpha(1-\gamma_5)v_{\bar{\nu}_{\ell_1}}, \qquad l_{\mathrm{C},\alpha}^{\mathrm{LNC}-} = \bar{u}_{\nu_{\ell_1}}\gamma_\alpha(1-\gamma_5)v_{\ell_1} = (l_{\mathrm{C},\alpha}^{\mathrm{LNC},+})^\dagger.
\end{aligned}
\tag{A6}
$$

and the functions $P_{D(C)_j}$ can be written as

$$
P_{D_j}^{\mathrm{LNV}} = \frac{1}{(k_N^2 - m_{N_j}^2) + i\Gamma_{N_j}m_{N_j}}, \qquad P_{C_j}^{\mathrm{LNV}} = \frac{1}{(k_N'^2 - m_{N_j}^2) + i\Gamma_{N_j}m_{N_j}},
\tag{A7}
$$

$$
P_{D_j}^{\mathrm{LNC}} = \frac{1}{m_{N_j}}P_{D_j}^{\mathrm{LNV}}, \qquad P_{C_j}^{\mathrm{LNC}} = \frac{1}{m_{N_j}}P_{C_j}^{\mathrm{LNV}}.
\tag{A8}
$$

where $k_N = q - p_1$ and $k_N' = q - p_2$ and $q = p - k$.

The matrix element mod-squared of the total amplitude, averaged over the initial spin and summed over the final spin is given by

$$
\begin{aligned}
|\bar{\mathcal{M}}_{\mathrm{tot}}^{\mathrm{Z},\pm}|^2 &= \frac{1}{2}\sum_{\mathrm{spins}}|\mathcal{M}_{\mathrm{tot}}^{\mathrm{Z},\pm}|^2 = \frac{1}{2}\sum_{\mathrm{spins}}|\sum_{j=1}^{2}(\mathcal{M}_{D_j}^{\mathrm{Z},\pm} + \mathcal{M}_{C_j}^{\mathrm{Z},\pm})|^2,\\
&= \frac{1}{2}\sum_{\mathrm{spins}}\left[\sum_{i,j=1}^{2}\mathcal{M}_{D_i}^{\mathrm{Z},\pm}(\mathcal{M}_{D_j}^{\mathrm{Z},\pm})^* + \sum_{i,j=1}^{2}\mathcal{M}_{C_i}^{\mathrm{Z},\pm}(\mathcal{M}_{C_j}^{\mathrm{Z},\pm})^* + \sum_{i,j=1}^{2}\mathcal{M}_{D_i}^{\mathrm{Z},\pm}(\mathcal{M}_{C_j}^{\mathrm{Z},\pm})^* + \sum_{i,j=1}^{2}\mathcal{M}_{C_i}^{\mathrm{Z},\pm}(\mathcal{M}_{D_j}^{\mathrm{Z},\pm})^*\right],\\
&= N\left[\sum_{i,j=1}^{2}v_{D_i}^{\mathrm{Z}\pm}(v_{D_j}^{\mathrm{Z}\pm})^* m_{N_i}m_{N_j}P_{D_i}^{\mathrm{Z}}(P_{D_j}^{\mathrm{Z}})^* T_{\mathrm{Z}}^{\pm}(DD^*) + \sum_{i,j=1}^{2}v_{D_i}^{\mathrm{Z}\pm}(v_{C_j}^{\mathrm{Z}\pm})^* m_{N_i}m_{N_j}P_{D_i}^{\mathrm{Z}}(P_{C_j}^{\mathrm{Z}})^* T_{\mathrm{Z}}^{\pm}(DC^*) + (D \leftrightarrow C)\right],
\end{aligned}
\tag{A9}
$$

where the sum over *spins* refers to the sum over spins of all external particles. The normalization constant is

$$
N = \frac{1}{2}G_F^4|V_{bq}|^2,
\tag{A10}
$$

and $T^{\mathrm{Z},\pm}(DD^*)^\pm$, $T^{\mathrm{Z},\pm}(CC^*)$, $T^{\mathrm{Z},\pm}(DC^*)$, $T^{\mathrm{Z},\pm}(D^*C)$ are given in following

$$
T_{\mathrm{Z}}^{\pm}(DD^*) = \sum_{\mathrm{spins}}[H_\nu^\pm(H_\rho^\pm)^*]\sum_{\mathrm{spins}}[L_{\mathrm{Z,}D}^{\nu\alpha\pm}(L_{\mathrm{Z,}D}^{\rho\beta\pm})^*]\sum_{\mathrm{spins}}[l_{\mathrm{D},\alpha}^{\mathrm{Z},\pm}(l_{\mathrm{D},\beta}^{\mathrm{Z},\pm})^*]
\tag{A11}
$$

$$T_{\rm Z}^{\pm}(CC^*) = \sum_{\rm spins}[H_\nu^{\pm}(H_\rho^{\pm})^*]\sum_{\rm spins}[L_{\rm Z,C}^{\alpha\nu\pm}(L_{\rm Z,C}^{\beta\rho\pm})^*]\sum_{\rm spins}[l_{{\rm C},\alpha}^{{\rm Z},\pm}(l_{{\rm C},\beta}^{{\rm Z},\pm})^*] \tag{A12}$$

$$T_{\rm Z}^{\pm}(DC^*) = \sum_{\rm spins}[H_\nu^{\pm}(H_\rho^{\pm})^*]\sum_{\rm spins}[L_{\rm Z,D}^{\nu\alpha\pm}(L_{\rm Z,C}^{\beta\rho\pm})^*]\sum_{\rm spins}[l_{{\rm D},\alpha}^{{\rm Z},\pm}(l_{{\rm C},\beta}^{{\rm Z},\pm})^*] \tag{A13}$$

$$T_{\rm Z}^{\pm}(D^*C) = \sum_{\rm spins}[(H_\nu^{\pm})^* H_\rho^{\pm}]\sum_{\rm spins}[(L_{\rm Z,D}^{\nu\alpha\pm})^* L_{\rm Z,C}^{\beta\rho\pm}]\sum_{\rm spins}[(l_{{\rm D},\alpha}^{{\rm Z},\pm})^* l_{{\rm C},\beta}^{{\rm Z},\pm}] \tag{A14}$$

From these above equations we get the following equality.

$$T_{\rm Z}(DD^*) \equiv T_{\rm Z}^{+}(DD^*) = T_{\rm Z}^{-}(DD^*), \qquad T_{\rm Z}(CC^*) \equiv T_{\rm Z}^{+}(CC^*) = T_{\rm Z}^{-}(CC^*) \tag{A15}$$

The total decay rates are given in Eqs. (2.4), (2.5), (2.7), and (2.8). With reference to the equations, the expressions of $\hat{\Gamma}_{\rm Z}^{\pm}(XY^*)_{ij}$ are given as

$$\hat{\Gamma}_{\rm Z}(XX^*)_{ij} = \frac{N}{2m_{\mathcal{B}1}}\int m_{N_i}m_{N_j}P_{X_i}^{Z}(P_{X_j}^{Z})^* T_{\rm Z}(XX^*)d\Phi_5, \qquad X = C, D. \tag{A16}$$

$$\hat{\Gamma}_{\rm Z}^{\pm}(XY^*)_{ij} = \frac{N}{2m_{\mathcal{B}1}}\int m_{N_i}m_{N_j}P_{X_i}^{Z}(P_{Y_j}^{Z})^* T_{\rm Z}^{\pm}(XY^*)d\Phi_5, \qquad X \neq Y = C, D. \tag{A17}$$

The five body phase space $d\Phi_5$ can be written as

$$d\Phi_5 \equiv d\Phi_5(\mathcal{B}_1 \to \mathcal{B}_2\ell_1\ell_2\ell_3\nu) = d\Phi_3(\mathcal{B}_1 \to \mathcal{B}_2\ell_1 N)\frac{dp_N^2}{2\pi}d\Phi_3(N \to \ell_2\ell_3\nu). \tag{A18}$$

APPENDIX B: THREE BODY DECAY OF $\mathcal{B}_1(p)(\to \mathcal{B}_2(k)\ell_1(p_1)N(p_N))$

With reference to the formula (2.10) the kinematics and the decay rate of $\mathcal{B}_1 \to \mathcal{B}_2\ell_1^- N$ in the following subsections.

1. Kinematics for $\mathcal{B}_1(p) \to \mathcal{B}_2(k)\ell_1(p_1)N(p_N)$

We do the kinematics in the $\mathcal{B}_1(b)$ rest frame (RF). In the $\mathcal{B}_1$-RF the $\mathcal{B}_2(c/u)$ and the first W^- boson with four momentum q fly in opposite direction. We say that the $\mathcal{B}_2$ travels in the $+\hat{z}$-direction so that the four momentum of the $\mathcal{B}_2$ and W^- are

$$k^{\mathcal{B}_1-\rm RF} \equiv (m_{\mathcal{B}_1} - E_q^{\mathcal{B}_1-\rm RF}, 0, 0, \mathbf{k}^{\mathcal{B}_1-\rm RF}), \tag{B1}$$

$$q^{\mathcal{B}_1-\rm RF} \equiv (E_q^{\mathcal{B}_1-\rm RF}, 0, 0, -\mathbf{k}^{\mathcal{B}_1-\rm RF}), \tag{B2}$$

where the q^0 and the $\mathbf{k}^{\mathcal{B}_1-\rm RF}$ are

$$E_q^{\mathcal{B}_1-\rm RF} = \frac{m_{\mathcal{B}_1}^2 + q^2 - m_{\mathcal{B}_2}^2}{2m_{\mathcal{B}1}},$$
$$|\mathbf{k}^{\mathcal{B}_1-\rm RF}| = \frac{\sqrt{\lambda(m_{\mathcal{B}_1}^2, m_{\mathcal{B}_2}^2, q^2)}}{2m_{\mathcal{B}1}}. \tag{B3}$$

In the first W^--RF the $\ell_1(p_1)$ and the $N(p_N)$ will decay back to back. We introduce an angle θ_1 made by ℓ_1 with respect to the $\mathcal{B}_2$, i.e., the $+\hat{z}$ direction. Hence the four moment of the ℓ_1 and the N in the $W^- - \rm RF$ are

$$p_1^{W^-\rm -RF} = (E_1^{W^-\rm -RF}, |\mathbf{p}_1^{W^-\rm -RF}|\sin\theta_1, 0, |\mathbf{p}_1^{W^-\rm -RF}|\cos\theta_1), \tag{B4}$$

$$p_N^{W^-\rm -RF} = \Big(\sqrt{q^2} - E_1^{W^-\rm -RF}, -|\mathbf{p}_1^{W^-\rm -RF}|\sin\theta_1, 0, -|\mathbf{p}_1^{W^-\rm -RF}|\cos\theta_1\Big), \tag{B5}$$

where $E_1^{W^-\rm -RF}$ and $\mathbf{p}_1^{W^-\rm -RF}$ are given as

$$E_1^{W^-\rm -RF} = \frac{q^2 + m_1^2 - p_N^2}{2\sqrt{q^2}}, \quad |\mathbf{p}_1^{W^-\rm -RF}| = \frac{\sqrt{\lambda(q^2, m_1^2, p_N^2)}}{2\sqrt{q^2}}. \tag{B6}$$

We will now boost back these two momentum from $W^- - \rm RF$ to $\mathcal{B}_1 - \rm RF$ using the following Lorentz boost matrix

$$\Lambda_{W^-\to\mathcal{B}_1} = \begin{pmatrix} \gamma_1 & -\gamma_1\beta_{1x} & -\gamma_1\beta_{1y} & -\gamma_1\beta_{1z} \\ -\gamma_1\beta_{1x} & 1+(\gamma_1-1)\frac{\beta_{1x}^2}{\vec{\beta}_1^2} & (\gamma_1-1)\frac{\beta_{1x}\beta_{1y}}{\vec{\beta}_1^2} & (\gamma_1-1)\frac{\beta_{1x}\beta_{1z}}{\vec{\beta}_1^2} \\ -\gamma_1\beta_{1y} & (\gamma_1-1)\frac{\beta_{1x}\beta_{1y}}{\vec{\beta}_1^2} & 1+(\gamma_1-1)\frac{\beta_{1y}^2}{\vec{\beta}_1^2} & (\gamma_1-1)\frac{\beta_{1y}\beta_{1z}}{\vec{\beta}_1^2} \\ -\gamma_1\beta_{1z} & (\gamma_1-1)\frac{\beta_{1x}\beta_{1z}}{\vec{\beta}_1^2} & (\gamma_1-1)\frac{\beta_{1y}\beta_{1z}}{\vec{\beta}_1^2} & 1+(\gamma_1-1)\frac{\beta_{1z}^2}{\vec{\beta}_1^2} \end{pmatrix} \tag{B7}$$

where the velocity $\vec{\beta}_1$ is the velocity of the $W^-(q)$ as seen in the $\mathcal{B}_1$-RF

$$\gamma_1 = \frac{1}{\sqrt{1-\vec{\beta}_1^2}}, \qquad \beta_{1x}=0, \qquad \beta_{1y}=0, \qquad \beta_{1z} = \frac{|\mathbf{k}^{\mathcal{B}_1-\mathrm{RF}}|}{E_q^{\mathcal{B}_1-\mathrm{RF}}}. \tag{B8}$$

The function $\lambda(a,b,c)$ is defined by, $\lambda(a,b,c) \equiv a^2+b^2+c^2-2ab-2ac-2bc$.

2. Matrix element and phase space for $\mathcal{B}_1(p) \to \mathcal{B}_2(k)\ell_1(p_1)N(p_N)$

Matrix element of $\mathcal{B}_1(b) \to \mathcal{B}(c/u)_2\ell_1^-N$ is written as

$$\mathcal{M}(\mathcal{B}_1 \to \mathcal{B}_2\ell_1^-N) = \frac{G_F}{\sqrt{2}} V_{bq}V_{\ell_1N}\bar{u}_{\ell_1}(p_1)\gamma^\mu(1-\gamma_5)v_N(p_N)H_\mu. \tag{B9}$$

Therefore the matrix mod square with average over initial baryon spin is given as

$$|\bar{\mathcal{M}}|^2 = \frac{1}{2}\sum_{\text{spins}}\mathcal{M}\mathcal{M}^* = \frac{1}{2}\frac{G_F^2}{2}|V_{bq}|^2|V_{\ell_1N}|^2 H_{\nu\rho}L^{\nu\rho}. \tag{B10}$$

Where hadronic tensor current $H_{\nu\rho}$ and leptonic tensor current $L_{\nu\rho}$ are given by

$$H_{\nu\rho} = \sum_{\text{spins}} H_\nu H_\rho^*, \qquad L_{\nu\rho} = 2\mathrm{tr}[\not{p}_1\gamma_\nu\not{p}_N\gamma_\rho(1-\gamma_5)]. \tag{B11}$$

Where the form of hadronic amplitude H_μ is given in A. The differential decay width for $\mathcal{B}_1 \to \mathcal{B}_2\ell_1^-N$ is given by

$$d\Gamma(\mathcal{B}_1 \to \mathcal{B}_2\ell_1^-N) = \frac{1}{2m_{\mathcal{B}1}} d\Phi_3(\mathcal{B}_1 \to \mathcal{B}_2\ell_1N)|\bar{\mathcal{M}}|^2. \tag{B12}$$

Where the three-body phase space is given by

$$\begin{aligned} d\Phi_3(\mathcal{B}_1 \to \mathcal{B}_2\ell_1N) &= \frac{d^3k}{2E_{\mathcal{B}_2}(\vec{p}_{\mathcal{B}_2})(2\pi)^3}\frac{d^3p_1}{2E_1(\vec{p}_1)(2\pi)^3}\frac{d^3p_N}{2E_N(\vec{p}_N)(2\pi)^3}(2\pi)^4\delta^4(p-k-p_1-p_N) \\ &= d\Phi_2(\mathcal{B}_1(p) \to \mathcal{B}_2(k)W^-(q))\frac{dq^2}{2\pi}d_2(W^-(q) \to \ell_1(p_1)N(p_N)). \end{aligned} \tag{B13}$$

Two particles phase space are given as follows.

$$d\Phi_2(\mathcal{B}_1(p) \to \mathcal{B}_2(k)W^-(q)) = \frac{1}{32\pi^2}\lambda^{1/2}\left(1, \frac{m_{\mathcal{B}2}^2}{m_{\mathcal{B}1}^2}, \frac{q^2}{m_{\mathcal{B}1}^2}\right)d\Omega_{\hat{q}} \tag{B14}$$

$$d\Phi_2(W^-(q) \to \ell_1(p_1)N(p_N)) = \frac{1}{32\pi^2}\lambda^{1/2}\left(1, \frac{m_1^2}{q^2}, \frac{m_N^2}{q^2}\right)d\Omega_{\hat{p_1}} \tag{B15}$$

Where $\hat{q}$ is the unit vector along the direction of $\vec{q}$ in the Λ_b^0 rest frame and $\hat{p_1}$ is the unit vector along the direction of $\vec{p_1}$ in the W^- rest frame. It is straightforward to show that $d\Omega_{\hat{q}} = 4\pi$ and $d\Omega_{\hat{p_1}} = 2\pi d\cos\theta_1$, and θ_1 is defined in the Appendix B 1. Here we get the following identities in the three body decay width between particle and antiparticle modes.

$$\Gamma(\mathcal{B}_1 \to \mathcal{B}_2\ell_1^-N) = \Gamma(\bar{\mathcal{B}}_1 \to \bar{\mathcal{B}}_2\ell_1^+\bar{N}), \Gamma(N \to \ell_2^-\ell_3^+\nu) = \Gamma(\bar{N} \to \ell_2^+\ell_3^-\nu) \tag{B16}$$

[1] Y. Fukuda *et al.* (Super-Kamiokande Collaboration), Evidence for Oscillation of Atmospheric Neutrinos, Phys. Rev. Lett. **81**, 1562 (1998).

[2] R. Wendell *et al.* (Super-Kamiokande Collaboration), Atmospheric neutrino oscillation analysis with sub-leading effects in Super-Kamiokande I, II, and III, Phys. Rev. D **81**, 092004 (2010).

[3] M. Ambrosio *et al.* (MACRO Collaboration), Atmospheric neutrino oscillations from upward through going muon multiple scattering in MACRO, Phys. Lett. B **566**, 35 (2003).

[4] R. N. Mohapatra and G. Senjanovic, Neutrino Mass and Spontaneous Parity Nonconservation, Phys. Rev. Lett. **44**, 912 (1980).

[5] J. Schechter and J. W. F. Valle, Neutrino masses in $SU(2) \times U(1)$ theories, Phys. Rev. D **22**, 2227 (1980).

[6] J. Schechter and J. W. F. Valle, Neutrino decay and spontaneous violation of lepton number, Phys. Rev. D **25**, 774 (1982).

[7] P. Minkowski, $\mu \to e\gamma$ at a rate of one out of 10^9 muon decays?, Phys. Lett. **67B**, 421 (1977).

[8] T. Yanagida, Horizontal gauge symmetry and masses of neutrinos, Conf. Proc. C **7902131**, 95 (1979).

[9] P. Ramond, The family group in grand unified theories, arXiv:hep-ph/9809459.

[10] S. L. Glashow, in edited by M. Levy *et al.*, Quarks and Leptons. Proceedings, Summer Institute, Cargese, France, NATO Science Series B, Vol. 61 (Springer, 1980), p. 707.

[11] W. Buchmuller, C. Greub, and P. Minkowski, Neutrino masses, neutral vector bosons and the scale of B-L breaking, Phys. Lett. B **267**, 395 (1991).

[12] T. Asaka, S. Blanchet, and M. Shaposhnikov, The nuMSM, dark matter and neutrino masses, Phys. Lett. B **631**, 151 (2005).

[13] F. del Aguila, J. A. Aguilar-Saavedra, J. de Blas, and M. Zralek, Looking for signals beyond the neutrino Standard Model, Acta Phys. Pol. B **38**, 3339 (2007).

[14] X. G. He, S. Oh, J. Tandean, and C. C. Wen, Large mixing of light and heavy neutrinos in seesaw models and the LHC, Phys. Rev. D **80**, 073012 (2009).

[15] J. Kersten and A. Y. Smirnov, Right-handed neutrinos at CERN LHC and the mechanism of neutrino mass generation, Phys. Rev. D **76**, 073005 (2007).

[16] A. Ibarra, E. Molinaro, and S. T. Petcov, TeV scale see-saw mechanisms of neutrino mass generation, the majorana nature of the heavy singlet neutrinos and $(\beta\beta)_{0\nu}$-decay, J. High Energy Phys. 09 (2010) 108.

[17] M. Nemevsek, G. Senjanovic, and Y. Zhang, Warm dark matter in low scale left-right theory, J. Cosmol. Astropart. Phys. 07 (2012) 006.

[18] A. Pilaftsis, Radiatively induced neutrino masses and large Higgs neutrino couplings in the standard model with Majorana fields, Z. Phys. C **55**, 275 (1992).

[19] H. Päs and W. Rodejohann, Neutrinoless double beta decay, New J. Phys. **17**, 115010 (2015).

[20] W. Rodejohann, Neutrino-less double beta decay and particle physics, Int. J. Mod. Phys. E **20**, 1833 (2011).

[21] S. Dell'Oro, S. Marcocci, M. Viel, and F. Vissani, Neutrinoless double beta decay: 2015 review, Adv. High Energy Phys. **2016**, 2162659 (2016).

[22] J. J. Gomez-Cadenas, J. Martin-Albo, M. Mezzetto, F. Monrabal, and M. Sorel, The search for neutrinoless double beta decay, Riv. Nuovo Cimento **35**, 29 (2012).

[23] M. Drewes and S. Eijima, Neutrinoless double β decay and low scale leptogenesis, Phys. Lett. B **763**, 72 (2016).

[24] T. Asaka, S. Eijima, and H. Ishida, On neutrinoless double beta decay in the νMSM, Phys. Lett. B **762**, 371 (2016).

[25] G. Cvetic, C. Dib, S. K. Kang, and C. S. Kim, Probing Majorana neutrinos in rare K and D, D_s, B, B_c meson decays, Phys. Rev. D **82**, 053010 (2010).

[26] J. C. Helo, S. Kovalenko, and I. Schmidt, Sterile neutrinos in lepton number and lepton flavor violating decays, Nucl. Phys. **B853**, 80 (2011).

[27] A. Atre, V. Barger, and T. Han, Upper bounds on lepton-number violating processes, Phys. Rev. D **71**, 113014 (2005).

[28] C. Dib, V. Gribanov, S. Kovalenko, and I. Schmidt, K meson neutrinoless double muon decay as a probe of neutrino masses and mixings, Phys. Lett. B **493**, 82 (2000).

[29] A. Ali, A. V. Borisov, and N. B. Zamorin, Majorana neutrinos and same sign dilepton production at LHC and in rare meson decays, Eur. Phys. J. C **21**, 123 (2001).

[30] J. M. Zhang and G. L. Wang, Lepton-number violating decays of heavy mesons, Eur. Phys. J. C **71**, 1715 (2011).

[31] H. Yuan, T. Wang, G. L. Wang, W. L. Ju, and J. M. Zhang, Lepton-number violating four-body decays of heavy mesons, J. High Energy Phys. 08 (2013) 066.

[32] R. M. Godbole, S. P. Maharathy, S. Mandal, M. Mitra, and N. Sinha, Interference effect in LNV and LNC meson decays for left right symmetric model, Phys. Rev. D **104**, 095009 (2021).

[33] B. Shuve and M. E. Peskin, Revision of the LHCb limit on Majorana neutrinos, Phys. Rev. D **94**, 113007 (2016).

[34] E. J. Chun, A. Das, S. Mandal, M. Mitra, and N. Sinha, Sensitivity of lepton number violating meson decays in different experiments, Phys. Rev. D **100**, 095022 (2019).

[35] S. Mandal, M. Mitra, and N. Sinha, Constraining the right-handed gauge boson mass from lepton number violating meson decays in a low scale left-right model, Phys. Rev. D **96**, 035023 (2017).

[36] A. Abada, V. De Romeri, M. Lucente, A. M. Teixeira, and T. Toma, Effective Majorana mass matrix from tau and pseudoscalar meson lepton number violating decays, J. High Energy Phys. 02 (2018) 169.

[37] A. Abada, C. Hati, X. Marcano, and A. M. Teixeira, Interference effects in LNV and LFV semileptonic decays: The Majorana hypothesis, J. High Energy Phys. 09 (2019) 017.

[38] J. Mejia-Guisao, D. Milanes, N. Quintero, and J. D. Ruiz-Alvarez, Exploring GeV-scale Majorana neutrinos in lepton-number-violating Λ_b^0 baryon decays, Phys. Rev. D **96**, 015039 (2017).

[39] G. Zhang and B. Q. Ma, Searching for lepton number violating Λ baryon decays mediated by GeV-scale Majorana neutrino with LHCb, Phys. Rev. D **104**, 9 (2021).

[40] G. Cvetič and C. S. Kim, Sensitivity bounds on heavy neutrino mixing $|U_{\mu N}|^2$ and $|U_{\tau N}|^2$ from LHCb upgrade, Phys. Rev. D **100**, 015014 (2019).

[41] C. Barbero, L. F. Li, G. López Castro, and A. Mariano, Matrix elements of four-quark operators and $\Delta L = 2$ hyperon decays, Phys. Rev. D **87**, 036010 (2013).

[42] S. Mandal and N. Sinha, Favoured B_c decay modes to search for a Majorana neutrino, Phys. Rev. D **94**, 033001 (2016).

[43] G. Moreno and J. Zamora-Saa, Rare meson decays with three pairs of quasi-degenerate heavy neutrinos, Phys. Rev. D **94**, 093005 (2016).

[44] G. Cvetic, C. S. Kim, R. Kogerler, and J. Zamora-Saa, Oscillation of heavy sterile neutrino in decay of $B \to \mu e \pi$, Phys. Rev. D **92**, 013015 (2015).

[45] G. Cvetic, C. Dib, C. S. Kim, and J. Zamora-Saa, Probing the Majorana neutrinos and their CP violation in decays of charged scalar mesons π, K, D, D_s, B, B_c, Symmetry **7**, 726 (2015).

[46] G. Cvetič, C. S. Kim, and J. Zamora-Saá, CP violation in lepton number violating semihadronic decays of K, D, D_s, B, B_c, Phys. Rev. D **89**, 093012 (2014).

[47] G. Cvetič, C. S. Kim, and J. Zamora-Saá, CP violations in $\pi^\pm$ meson decay, J. Phys. G **41**, 075004 (2014).

[48] C. S. Kim, G. López Castro, and D. Sahoo, Constraints on a sub-eV scale sterile neutrino from nonoscillation measurements, Phys. Rev. D **98**, 115021 (2018).

[49] C. S. Kim, Y. Kwon, D. Lee, S. Oh, and D. Sahoo, Probing sterile neutrinos in $B(D)$ meson decays at Belle II (BESIII), Eur. Phys. J. C **80**, 730 (2020).

[50] D. Milanés and N. Quintero, Search for lepton-number-violating signals in the charm sector, Phys. Rev. D **98**, 096004 (2018).

[51] J. Mejia-Guisao, D. Milanés, N. Quintero, and J. D. Ruiz-Alvarez, Lepton number violation in B_s meson decays induced by an on-shell Majorana neutrino, Phys. Rev. D **97**, 075018 (2018).

[52] D. Milanes, N. Quintero, and C. E. Vera, Sensitivity to Majorana neutrinos in $\Delta L = 2$ decays of B_c meson at LHCb, Phys. Rev. D **93**, 094026 (2016).

[53] G. L. Castro and N. Quintero, Bounding resonant Majorana neutrinos from four-body B and D decays, Phys. Rev. D **87**, 077901 (2013).

[54] N. Quintero, G. Lopez Castro, and D. Delepine, Lepton number violation in top quark and neutral B meson decays, Phys. Rev. D **84**, 096011 (2011); Erratum, Phys. Rev. D **86**, 079905 (2012).

[55] L. S. Littenberg and R. E. Shrock, Upper bounds on Delta L = 2 decays of baryons, Phys. Rev. D **46**, R892 (1992).

[56] C. Barbero, G. Lopez Castro, and A. Mariano, Double beta decay of Sigma- hyperons, Phys. Lett. B **566**, 98 (2003).

[57] G. Cvetic and C. S. Kim, Sensitivity limits on heavy-light mixing $|U_{\mu N}|^2$ from lepton number violating B meson decays, Phys. Rev. D **96**, 035025 (2017); Erratum, Phys. Rev. D **102**, 019903 (2020); Erratum, Phys. Rev. D **102**, 039902 (2020).

[58] G. Cvetic, C. S. Kim, S. Mendizabal, and J. Zamora-Saa, Exploring CP-violation, via heavy neutrino oscillations, in rare B meson decays at Belle II, Eur. Phys. J. C **80**, 1052 (2020).

[59] D. Das and J. Das, CP violation with a GeV-scale Majorana neutrino in $\Lambda_b \to (\Lambda_c^+, p^+)\pi^+\mu^-\mu^-$ decays, Phys. Rev. D **103**, 073001 (2021).

[60] G. Lopez Castro and N. Quintero, Lepton number violating four-body tau lepton decays, Phys. Rev. D **85**, 076006 (2012); Erratum, Phys. Rev. D **86**, 079904 (2012).

[61] C. Dib, J. C. Helo, M. Hirsch, S. Kovalenko, and I. Schmidt, Heavy sterile neutrinos in tau decays and the MiniBooNE anomaly, Phys. Rev. D **85**, 011301 (2012).

[62] H. Yuan, Y. Jiang, T. h. Wang, Q. Li, and G. L. Wang, Testing the nature of neutrinos from four-body τ decays, J. Phys. G **44**, 115002 (2017).

[63] J. Zamora-Saa, Resonant CP violation in rare $\tau^\pm$ decays, J. High Energy Phys. 05 (2017) 110.

[64] C. S. Kim, G. López Castro, and D. Sahoo, Discovering intermediate mass sterile neutrinos through $\tau^- \to \pi^-\mu^- e^+\nu$ (or $\bar{\nu}$) decay, Phys. Rev. D **96**, 075016 (2017).

[65] A. Abada, J. Kriewald, and A. M. Teixeira, On the role of leptonic CPV phases in cLFV observables, Eur. Phys. J. C **81**, 1016 (2021).

[66] A. Das, P. S. B. Dev, and C. S. Kim, Constraining sterile neutrinos from precision Higgs data, Phys. Rev. D **95**, 115013 (2017).

[67] A. Das, Y. Gao, and T. Kamon, Heavy neutrino search via semileptonic Higgs decay at the LHC, Eur. Phys. J. C **79**, 424 (2019).

[68] A. Das and N. Okada, Bounds on heavy Majorana neutrinos in type-I seesaw and implications for collider searches, Phys. Lett. B **774**, 32 (2017).

[69] G. Cvetič, A. Das, S. Tapia, and J. Zamora-Saá, Measuring the heavy neutrino oscillations in rare W boson decays at the Large Hadron Collider, J. Phys. G **47**, 015001 (2020).

[70] G. Cvetič, A. Das, and J. Zamora-Saá, Probing heavy neutrino oscillations in rare W boson decays, J. Phys. G **46**, 075002 (2019).

[71] B. Fuks, J. Neundorf, K. Peters, R. Ruiz, and M. Saimpert, Probing the Weinberg operator at colliders, Phys. Rev. D **103**, 115014 (2021).

[72] B. Fuks, J. Neundorf, K. Peters, R. Ruiz, and M. Saimpert, Majorana neutrinos in same-sign $W^\pm W^\pm$ scattering at the LHC: Breaking the TeV barrier, Phys. Rev. D **103**, 055005 (2021).

[73] Y. Cai, T. Han, T. Li, and R. Ruiz, Lepton number violation: Seesaw models and their collider tests, Front. Phys. **6**, 40 (2018).

[74] R. Ruiz, A quantitative study on helicity inversion in Majorana neutrino decays at the LHC, Phys. Rev. D **103**, 015022 (2021).

[75] F. Najafi, J. Kumar, and D. London, CP violation in rare lepton-number-violating W decays at the LHC, J. High Energy Phys. 04 (2021) 021.

[76] S. Bray, J. S. Lee, and A. Pilaftsis, Resonant CP violation due to heavy neutrinos at the LHC, Nucl. Phys. **B786**, 95 (2007).

[77] R. Aaij *et al.* (LHCb Collaboration), Search for Majorana Neutrinos in $B^- \to \pi^+\mu^-\mu^-$ Decays, Phys. Rev. Lett. **112**, 131802 (2014).

[78] J. R. Batley *et al.* (NA48/2 Collaboration), Searches for lepton number violation and resonances in $K^\pm \to \pi\mu\mu$ decays, Phys. Lett. B **769**, 67 (2017).

[79] C. O. Dib, M. Campos, and C. S. Kim, CP violation with Majorana neutrinos in K meson decays, J. High Energy Phys. 02 (2015) 108.

[80] D. Rajaram *et al.* (HyperCP Collaboration), Search for the Lepton-Number-Violating Decay $\Xi \to p\mu^-\mu^-$, Phys. Rev. Lett. **94**, 181801 (2005).

[81] K. Kodama *et al.* (E653 Collaboration), Upper limits of charm hadron decays to two muons plus hadrons, Phys. Lett. B **345**, 85 (1995).

[82] M. Ablikim *et al.* (BESIII Collaboration), Search for the lepton number violating decay $\Sigma^- \to pe^-e^-$ and the rare inclusive decay $\Sigma^- \to \Sigma^+ X$, Phys. Rev. D **103**, 052011 (2021).

[83] C. Giunti and C. W. Kim, Fundamentals of Neutrino Physics And Astrophysics (2022).

[84] A. G. Cohen, S. L. Glashow, and Z. Ligeti, Disentangling neutrino oscillations, Phys. Lett. B **678**, 191 (2009).

[85] W. Detmold, C. Lehner, and S. Meinel, $\Lambda_b \to p\ell^-\bar{\nu}_\ell$ and $\Lambda_b \to \Lambda_c\ell^-\bar{\nu}_\ell$ form factors from lattice QCD with relativistic heavy quarks, Phys. Rev. D **92**, 034503 (2015).

[86] A. Atre, T. Han, S. Pascoli, and B. Zhang, The search for heavy Majorana neutrinos, J. High Energy Phys. 05 (2009) 030.

[87] D. Liventsev *et al.* (Belle Collaboration), Search for heavy neutrinos at Belle, Phys. Rev. D **87**, 071102 (2013); Erratum, Phys. Rev. D **95**, 099903 (2017).

[88] O. Adriani *et al.* (L3 Collaboration), Search for isosinglet neutral heavy leptons in Z0 decays, Phys. Lett. B **295**, 371 (1992).

[89] P. Abreu *et al.* (DELPHI Collaboration), Search for neutral heavy leptons produced in Z decays, Z. Phys. C **74**, 57 (1997); Erratum, Z. Phys. C **75**, 580 (1997).

[90] J. Badier *et al.* (NA3 Collaboration), Direct photon production from pions and protons at 200-GeV/c, Z. Phys. C **31**, 341 (1986).

[91] P. Vilain *et al.* (CHARM II Collaboration), Search for heavy isosinglet neutrinos, Phys. Lett. B **343**, 453 (1995).

[92] A. Vaitaitis *et al.* (NuTeV and E815 Collaborations), Search for Neutral Heavy Leptons in a High-Energy Neutrino Beam, Phys. Rev. Lett. **83**, 4943 (1999).

[93] R. Aaij *et al.* (LHCb Collaboration), Differential branching fraction and angular analysis of $\Lambda_b^0 \to \Lambda\mu^+\mu^-$ decays, J. High Energy Phys. 06 (2015) 115; Erratum, J. High Energy Phys. 09 (2018) 145.

[94] R. Aaij *et al.* (LHCb Collaboration), Angular moments of the decay $\Lambda_b^0 \to \Lambda\mu^+\mu^-$ at low hadronic recoil, J. High Energy Phys. 09 (2018) 146.